skeletal actin, α-cardiac actin, myosin light chain-2v (MLC-2v), MLC-2a, Cav1.2, myoD, calponin, and α-smooth muscle actin genes. The primers and PCR cycles used were as described previously [6,15,16]. Primers for Cav1.2 were CTGCAGGTGATGATGAGGTC for the forward primer and GCGGTGTTGTTGGCGTTGTT for the reverse primer.

2.9. Immunostaining

Cells were attached to gelatin-coated glass slides, fixed in 4% paraformaldehyde, and then stained with primary antibodies against anti-GATA4, anti-troponin I, and anti-MEF2C antibodies (all from Santa Cruz Biotechnology), or anti-connexin43 antibody (Sigma). Anti-goat-IgG conjugated with Texas red or anti-rabbit IgG conjugated with Rhodamine (1:500, Pharmingen) was use as a secondary antibody.

2.10. Action potential recording

Electrophysiological studies were performed in IMDM containing (mmol/L) $CaCl_2$ 1.49, KCl 4.23, and HEPES 25 (pH 7.4). Cultured cells were placed on the stage of an inverted phase contrast optic (Diaphoto-300, Nikon) at 23 °C. Action potentials were recorded using conventional microelectrodes as described previously [8]. Intracellular recordings were taken from MLC2v-EGFP-purified cells 3 weeks following transfection.

2.11. Cell transplantation

Animal Care and Use Committees of Keio University approved all experimental procedures and protocols. Female scid mice (12 weeks) were anesthetized initially with ether and placed on a warm pad maintained at 37 °C. The trachea was cannulated with a polyethylene tube connected to a respirator (Shinano, Tokyo, Japan) with a tidal volume set at 0.6 ml and a rate set at 110/min. Mice were then anesthetized with 0.5–1.5% isoflurene under controlled ventilation with a respirator for the remainder of the surgical procedure. A left thoracotomy was performed between ribs 4 and 5, and the pericardial sac was removed. Isolated EGFP(+) cells that had been expanded for 5 days were resuspended in PBS at a concentration of 5×10^7 cells/ml. A total cell suspension volume of 50 μl was drawn into a 50 μl Hamilton syringe with a 31-gauge needle, and 10 μl was injected into the anterior wall of the left ventricle. Following the transplantation, residual cells in the syringe were collected and stained with trypan blue. The total and living cell numbers were counted. The number of living cells to inject was calculated by the following formula. (The injected living cells)=[(Total injected cells)−(Residual cells in the syringe)](Percent of living cells). Injection of PBS was used as a control.

2.12. Histological studies

The mice were sacrificed, and the hearts were dissected and fixed in 2% formaldehyde and 0.2% glutaraldehyde in PBS at room temperature for 5 min. The hearts were then washed in PBS and then incubated overnight in X-gal solution (1 mg/ml X-gal, 15 mmol/L potassium ferricyanide, 15 mmol/L potassium ferrocyanide, and 2 mmol/L $MgCl_2$ in PBS). The hearts were refixed in the same fix solution, embedded in paraffin, and sectioned into 6-μm-thick slices for hematoxylin–eosin staining. The numbers of X-gal-stained CMG cells were counted using serial sections of the transplanted heart (more than 200 slices/mouse), and an estimate of total transplanted cell survival was obtained using the following formula. (Percent of cells surviving in the recipient heart)=[(Total surviving cells in the recipient heart)/(Injected living cells)]100.

To observe EGFP fluorescence, the hearts were embedded in OCT compound and frozen with liquid nitrogen. A cryostat was used to generate 6-μm-thick sections. The samples were examined with a confocal LASER microscope (LSM510; Carl Zeiss, Jena, Germany). The GFP signal was confirmed by emission finger printing, using the LSM 510 Meta spectrometer (Carl Zeiss).

2.13. Electrocardiography (ECG) recording

ECG recordings were performed 2 and 4 weeks after transplantation. Mice were anesthetized with ether, needle limb leads were fixed, and the ECG was recorded for 1 h.

2.14. Statistics

Values are presented as mean±SD. The significance of differences among mean values was determined by ANOVA. Statistical comparison of the control and treated groups was carried out using the nonparametric Fisher's multiple comparison tests. The level accepted for significance was $p<0.05$.

3. Results

3.1. Regenerated cardiomyocytes, but not other cell types, express EGFP

G418-resistant cells were exposed to 5-azacytidine and after 3 days EGFP(+) cells exhibited a fibroblast-like morphology (Fig. 1b,c), and were difficult to distinguish from other cell types. After 7 days, the EGFP(+) cells displayed a spindle-like morphology (Fig. 1d,e), but did not spontaneously beat at this stage. After 3 weeks, the EGFP(+) cells began to appear more rod-like and form inter-cell connections and after 4 weeks spontaneous beating was observed (Fig. 1f,g). Some fractions of the EGFP(−)

cells differentiated into adipocytes, but other EGFP(−) cells did not display any specific morphology. These findings indicate that the MLC2v–EGFP system may be a useful method for distinguishing regenerated cardiomyocytes from other cell types at an early stage.

3.2. Fluorescence-activated cell sorting (FACS) analysis

FACS analysis was performed 3 day after 5-azacytidine exposure to isolate regenerated cardiomyocytes. Control cells (before 5-azacytidine exposure) showed no detectable fluorescence (Fig. 2a), whereas 3 days after 5-azacytidine exposure the cells stable transfected with the MLC2v-EGFP expression plasmid generated sufficient EGFP signal for cell sorting (Fig. 2b). The EGFP(+) fraction ranged from 6–24%. Fig. 2c,d shows the cells 4 days after cell sorting (7 days after 5-azacytidine exposure) displaying a fibroblast-like morphology. The percentage of EGFP-positive cells was calculated by comparing cell counts from phase contrast microscopy with EGFP(+) cell counts using fluorescence microscopy, 3 days after cell sorting. More than 99% of the sorted cells expressed EGFP fluorescence. After 3 weeks, these cells had a spindle-like appearance and began spontaneous beating (Fig. 2e,f).

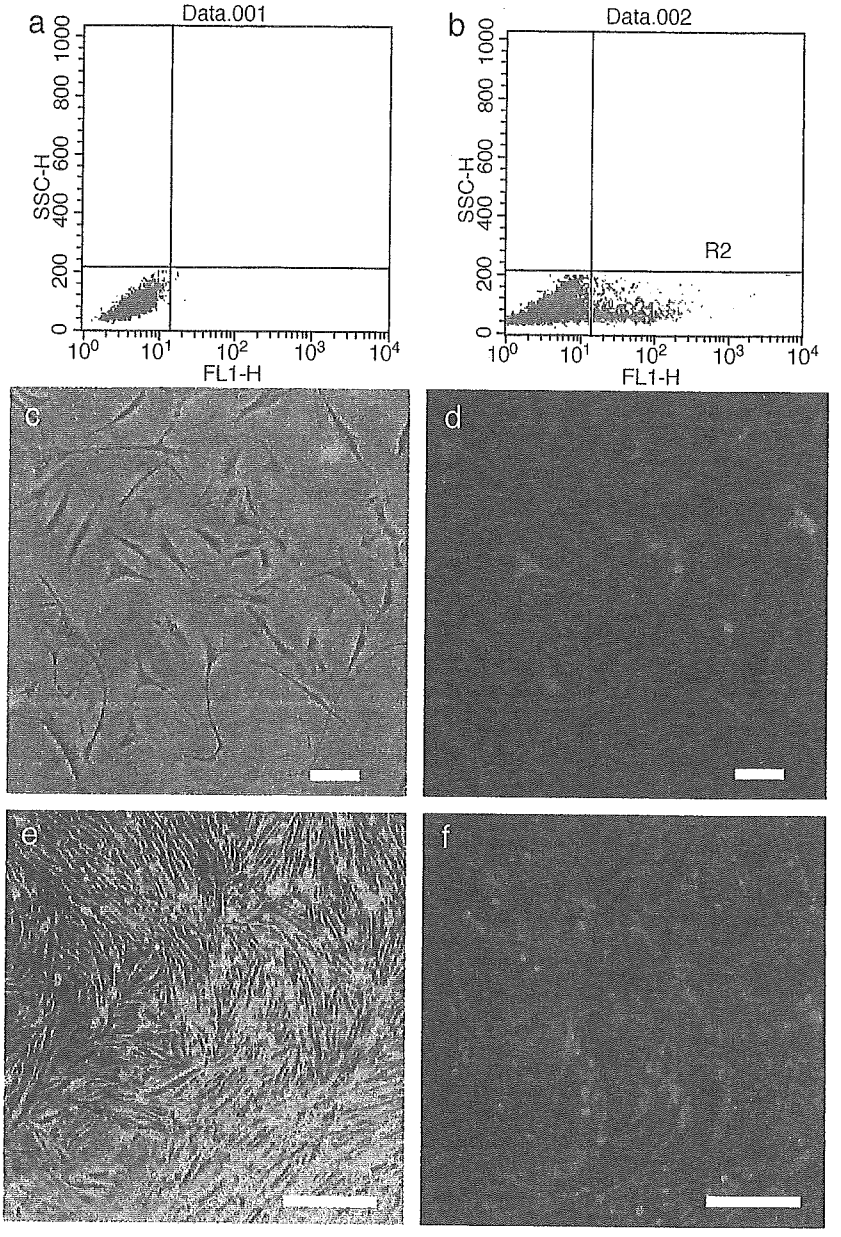

Fig. 2. FACS analysis of the pMLC-2v-EGFP-transfected cells and microscopy of the sorted cells. (a, b) FACS analysis of the pMLC-2v-EGFP-transfected cells. The horizontal axis indicates the intensity of EGFP fluorescence. (a) Control cells, (b) cells 3 days after exposure to 5-azacytidine exposure. d and f are fluorescence microscopy images of the EGFP signal. c and e are phase contrast microscopy views of the same field. (c, d) 4 days, and (e, f) 3 weeks after cell sorting. Note that all the cells display EGFP fluorescence, and that the EGFP(+) CMG cells exhibit a cardiomyocyte-like appearance and spontaneously beat after 3 weeks. Bars in c,d and e,f indicate 100 and 500 μm, respectively.

3.3. Character of the sorted EGFP(+) regenerated cardiomyocytes

A total of 768 single EGFP(+) cell clones were isolated using FACS analysis. Although EGFP(+) cells undergo cell division after 5-azacytidine exposure, a cardiomyocyte cell line could not be generated as cells stop proliferating after several cell divisions. The cells were exposed to BrdU to confirm their mitogenicity, and double immunostaining was performed with antisarcomeric myosin and anti-BrdU antibodies. Myosin-positive cells incorporated BrdU until day 5, but stopped incorporating it after day 7 (Fig. 3a). This finding shows that the mitogenicity of the isolated EGFP(+) CMG cells is limited, so it can be assumed that the risk of cardiomyosarcoma formation is negligible.

RT-PCR analysis of cardiac contractile proteins revealed that the isolated EGFP(+) CMG predominantly express the β-myosin heavy chain, α-skeletal-actin, and MLC-2v, indicating that the phenotype of these cells represents fetal ventricular cardiomyocytes. These cells also express cardiac L-type Ca^{2+} channels but did not express myogenic genes such as myoD, or smooth-muscle-specific genes, such as calponin or α-smooth muscle actin genes (Fig. 3b).

3.4. Action potential recording

MLC2v-EGFP-selected cells showed regular spontaneous beating 3 weeks following selection. The action potentials of these cells had a relatively shallow resting membrane potential with a late diastolic slow depolarization, like a pacemaker potential. They also displayed peak-notch-plateau characteristics representative of ventricular cardiomyocyte-like action potentials (Fig. 3c).

3.5. Immunostaining and transmission electron microscopy

Immunostaining revealed that EGFP(+) but not EGFP(−) CMG cells express cardiac troponin I (Fig. 4a–d). EGFP(+) CMG cells express both GATA4 and MEF2C, respectively (Fig. 4e,f). Interestingly, EGFP(−) CMG cells express GATA4 and Nkx2.5. These findings are consistent with the previous report that these cardiac transcription factors are expressed before final 5-azacytidine exposure [6]. EGFP(+) CMG cells also express connexin43 (Fig. 4g).

The sorted GFP(+) cells were cultured for 2 weeks, fixed, and processed for transmission electron microscopy. The typical contractile apparatus of the sarcomeres, including striation pattern, was observed (Fig. 4h).

3.6. Cell transplantation study

Animals with transplanted EGFP(+) cells were sacrificed at 2, 4, 8, and 12 weeks. Confocal LASER microscopy revealed that the EGFP(+) transplanted cardiomyocytes survived in the recipient heart (Fig. 5a–c). The control experiment revealed no EGFP(+) transplanted cardiomyocytes (data not shown) [17]. The orientation of the transplanted cells was consistent with the cardiomyocytes of the recipient heart. The EGFP(+) cells were observed only at the site of injection in the left ventricle and in no other parts of the heart. We also confirmed that these green signals were

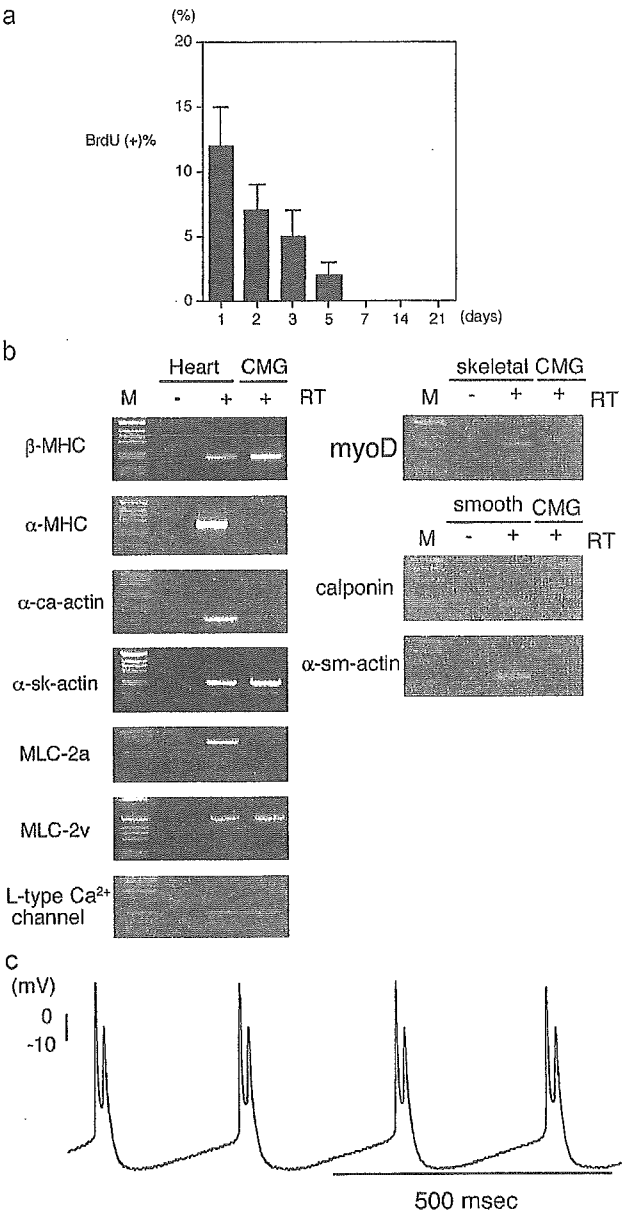

Fig. 3. Characteristics of the sorted CMG cardiomyocytes. (a) BrdU incorporation of EGFP(+) CMG cells after cell sorting. BrdU was loaded for 5 h, and its incorporation was detected. BrdU incorporation was observed until 5 days after cell sorting (8 days after 5-azacytidine exposure). (b) Phenotype of the EGFP(+) CMG cells. RT-PCR was performed for α-MHC, β-MHC, MLC-2v, MLC-2a, α-skeletal actin, α-cardiac actin, and cardiac α1c Ca^{2+} channel. The expression pattern of the cardiac contractile protein indicated that these cells had the fetal ventricular phenotype. MLC-2v-EGFP selected cells did not express myoD, calponin, and α-smooth muscle actin genes. Femoral muscle, which includes vascular smooth muscle cells, were used as a positive control. M: 1-kb DNA ladder. RT: reverse transcription. (c) The representative tracing of the action potentials at 3 weeks after cell sorting was shown. These action potentials show ventricular cardiomyocyte-like action potentials.

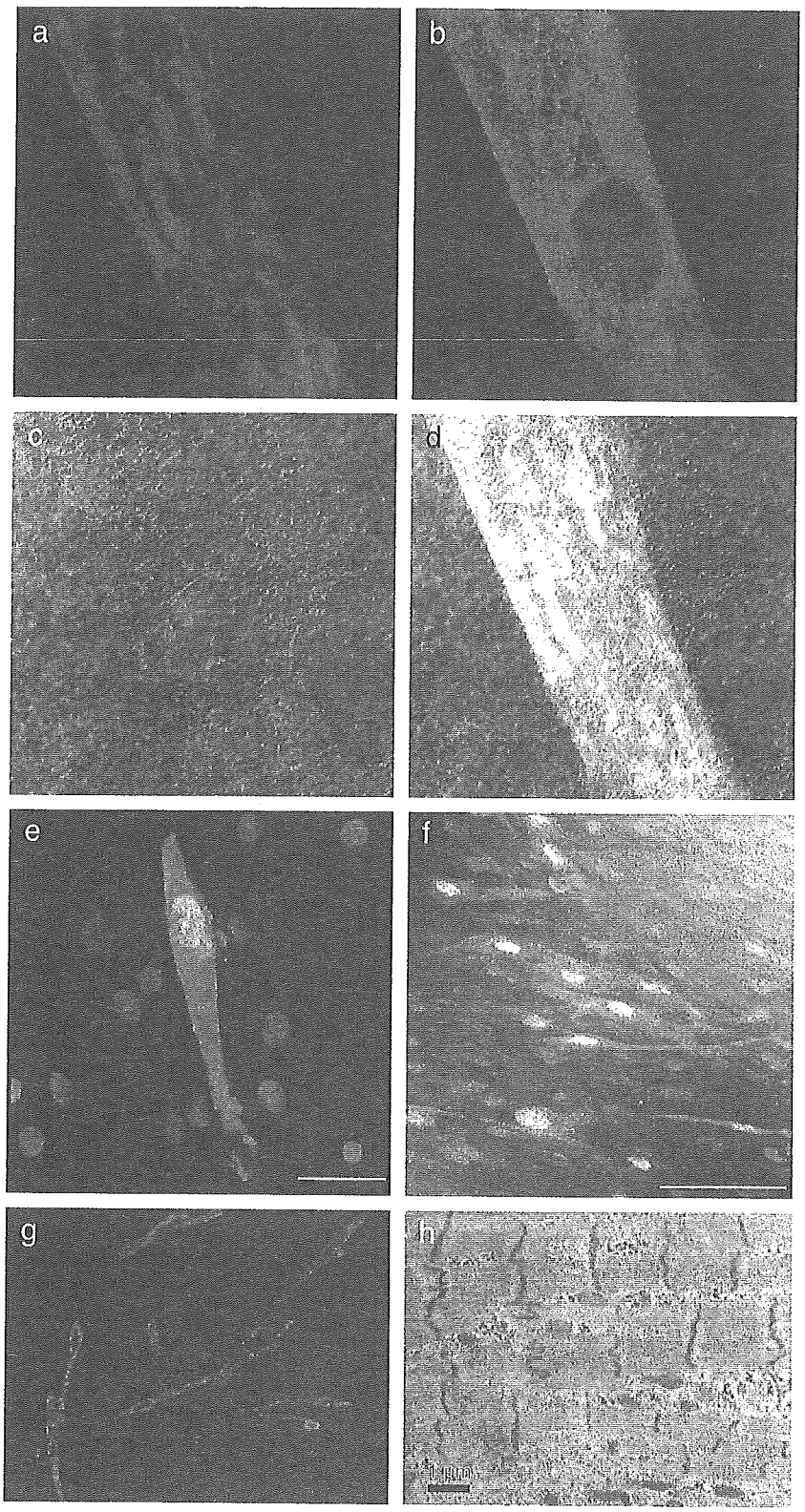

Fig. 4. Photograph of immunofluorescence and transmission electron micrograph of CMG cells. (a–d) EGFP(+) and EGFP(−) CMG cells were stained with anti-troponin I antibodies (a) and DAPI (c). EGFP(+) CMG cells expressed troponin I, but EGFP(−) CMG cell did not express troponin I. (e) Immunofluorescent staining with GATA4. Both EGFP(+) and EGFP(−) CMG cells expressed GATA4. (f) Immunofluorescent staining with MEF2C. Both EGFP(+) and EGFP(−) CMG cells expressed MEF2C. (g) Immunofluorescent staining with connexin43. EGFP(+) CMG cells expressed connexin43. (h) Transmission electron microscopy of the CMG cells showed typical contractile apparatus.

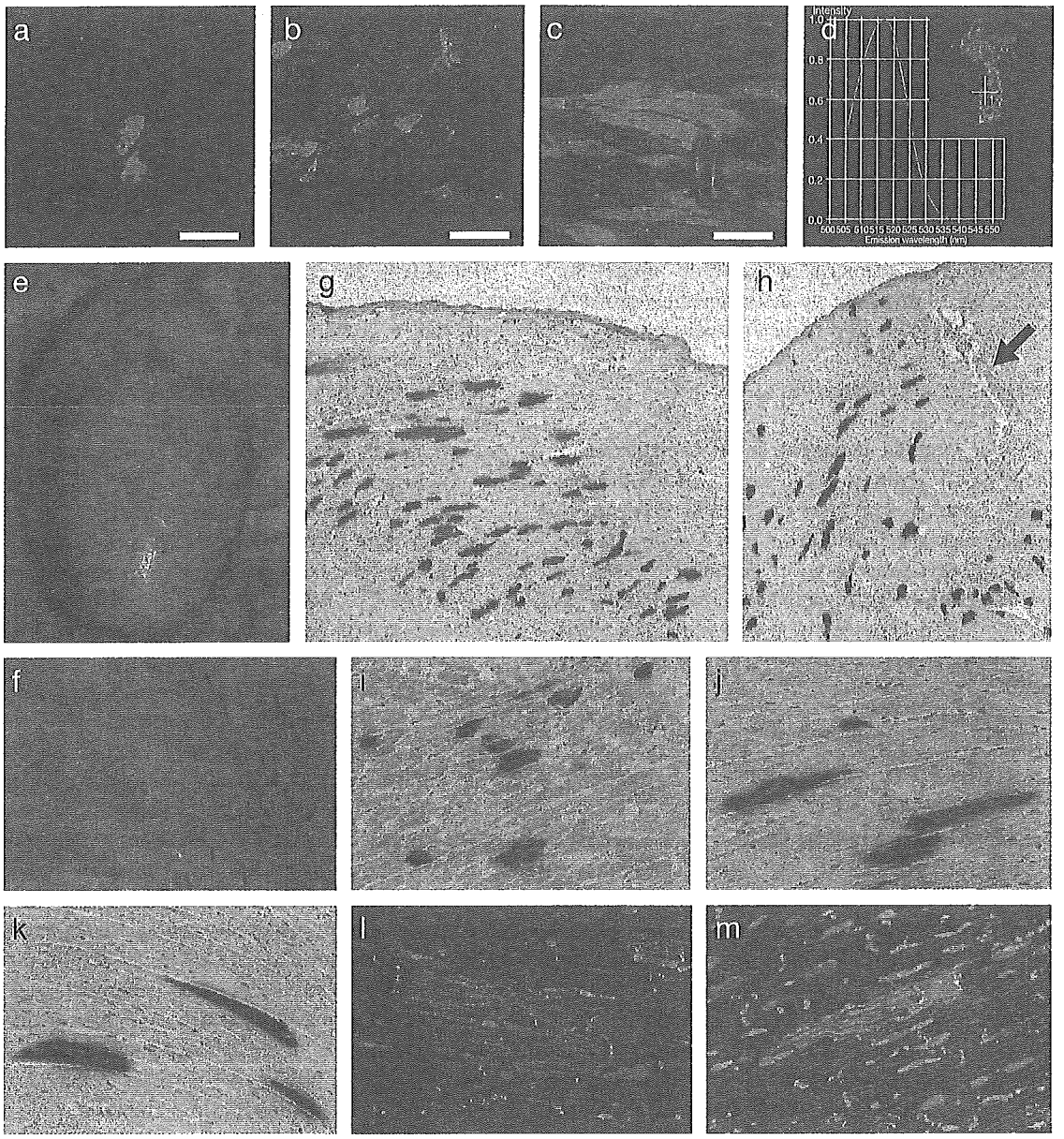

Fig. 5. Histological analysis of the transplanted CMG cells. (a–c) Confocal microscopy of the recipient heart transplanted with the sorted cardiomyocytes at 4 weeks. The transplanted cells could be clearly identified by EGFP signals. a and b show the transverse section of the transplanted cardiomyocytes, and c shows the longitudinal section. Bars indicate 50 μm. (d) The emission profile of the green signal in GFP^+ cells was investigated by CLSM. The emission peak existed at 510–530 nm, and the profile was ascertained to be that of GFP, and not arising from nonspecific background. The inset shows the GFP^+ transplanted cells, and the cross indicates the site of the emission profile. (e–m) The bone-marrow-derived cardiomyocytes were sorted and marked with adenovirus-mediated LacZ gene. e is a photograph of the whole heart, and f shows an enlarged photograph of the injected site. The transplanted LacZ-positive cells were identified from the surface. g and h show the microscopy of the injected site of the left ventricle. The samples were stained with LacZ and hematoxylin–eosin. i–k show higher magnification of the same fields: i shows the transverse section, and j,k show the longitudinal section. (l, m) Transplanted CMG cells were stained with anticonnexin43 antibody and DAPI. Connexin43 was expressed at the both ends of the transplanted EGFP(+) CMG cells. Green: EGFP, Blue: DAPI, Red: connexin43.

not due to nonspecific background fluorescence, but due to the EGFP itself, using absorbance frequency analysis on a LSM510 Meta spectrometer (Fig. 5d).

Fig. 5e shows the entire murine heart stained with LacZ at 4 weeks after transplantation, and Fig. 5f showed an enlarged photograph of the site of injection. Cells were transplanted into the anterior free wall of the left ventricle and were observed to be rectangular in shape and located at the surface of the heart. Fig. 5g,h shows the site of injection in a transverse section of the left ventricle stained with LacZ and hematoxylin–eosin 4 weeks after transplantation. The scar of the injection needle is shown in Fig. 5h. Granulomatous tissue was also observed around the site of injection. The LacZ-stained transplanted cells were clearly visible, and were located throughout the site of injection. Fig. 5i–k shows transverse and longitudinal sections of the transplanted cardiomyocytes at higher magnifications. This figure clearly shows the arrangement of the transplanted

cells parallel to the cardiomyocytes of the recipient heart. Fig. 5l,m shows expression of connexin43 at the longitudinal border between transplanted EGFP(+) CMG cells and adjacent cardiomyocytes of the recipient heart.

Transplanted cardiomyocytes survived in the recipient heart for more than 3 months and the estimated percentage of cells surviving transplantation was 6.5±3.2%. Table 1 shows the diameter of transplanted cardiomyocytes in transverse section. The diameter increased to almost the same size as the cardiomyocytes in the recipient heart over 4 weeks after which time no further increase was observed.

3.7. ECG recording and survival curve

Of the 35 mice that had undergone cell transplantation, 5 died within 24 h. This is most likely a result of the surgical procedure. The remaining 30 mice survived the duration of the observation period. ECGs recordings in 5 mice at 2 and 4 weeks, respectively, showed no evidence of arrhythmia (ventricular premature beats, ventricular tachycardia) during the recording period (data not shown). This finding suggests that survival of recipients in this model is not affected by arrhythmia.

4. Discussion

Since our report that cardiomyocytes can be regenerated from bone marrow stem cells [6,7], several studies have shown that transplantation of bone-marrow mononuclear cells or bone marrow stem cell fractions into the heart can improve cardiac function. Although the direct transplantation of these cells omits prior differentiation or purification, and thereby shortens the therapeutic period, it remains undetermined whether transplanted cells differentiate into the desired cardiomyocytes or endothelial cells, and not into other cell types including osteoblasts, chondroblasts, or adipocytes. The establishment of a reliable method to repair injured myocardium using cardiomyocyte transplantation requires the preparation of a sufficient number of well-characterized, purified regenerated cardiomyocytes, and an estimation of the survival rate of the transplanted cells.

Tomita [18] reported that the transplantation of 5-azacytidine-treated primary cultured marrow-stromal cells improved the function of the infarcted myocardium. Since the population of mesenchymal stem cells in primary cultured mice marrow stromal cells is less than 0.01%, it is likely that most of the cells transplanted do not differentiate into cardiomyocytes, and that the observed improvement in cardiac function is caused by an improvement in ventricular remodeling or stimulation of angiogenesis.

Jackson transplanted adult stem cells [CD34(−)/low, c-Kit(+), Sca-1(+)] into lethally irradiated mice subsequently rendered ischemic by coronary artery occlusion followed by reperfusion, and reported that the engrafted cells migrated into ischemic cardiac muscle and blood vessels, differentiated to cardiomyocytes and endothelial cells, and contributed to the formation of functional tissue [19]. They found that the donor-derived endothelial cells were present at around 3.3%, primarily in small vessels adjacent to the infarct, and that donor-derived cardiomyocytes were present at around 0.02% and were found primarily in the peri-infarct region. Taken together, these findings show that differentiation from marrow stromal cells to cardiomyocytes in vivo is possible, but that their prevalence is less than other cell types. Condrelli [20] reported that neural stem cells differentiated into heart muscle cells when mixed with heart muscle cells from newborn rats in a process known as transdifferentiation. The mechanism of in vitro transdifferentiation is based on the idea that the developmental limitations of tissue specific stem cells are dictated by the environment, and that new signals that relax these limitations may be provided by cells from a different tissue [20].

It is most likely that the direct transplantation of stem cells into the heart does not facilitate their differentiation into cardiomyocytes, but merely results in their fusion with residual cardiomyocytes. We propose a more rigorous method to achieve repair of damaged tissue by first differentiation adult stem cells cardiomyocytes in vitro, and then transplanting a sufficient number of differentiated cardiomyocytes into the damaged heart tissue. To avoid possible adverse effects, we emphasize the importance of thoroughly investigating the molecular and electrophysiological characteristics of the stem cell-derived regenerated cardiomyocytes prior to transplantation.

In the present study, we used an EGFP reporter gene under the control of the MLC-2v promoter to tag isolated cardiomyocytes. Following FACS analysis, 99% of the isolated cardiomyocytes expressed EGFP, and when transplanted into the recipient heart they survived for at least 4 weeks. We observed no other cell types in the transplanted area, but this may have been because we only used a strongly expressing EGFP(+) fraction.

Table 1
Diameter of the transplanted bone-marrow-derived cardiomyocyte

Time after transplantation (weeks)	2	4	8	12	Recipient cardiomyocytes
Diameter (μm)	10.5±3.6*	19.0±4.8$	19.1±5.0$	19.1±4.9$	19.5±5.1

The diameter of the transplanted cardiomyocytes was measured by the transverse section of the recipient hearts. Each data was obtained by measuring 200 cells. Mean±SD. $: not significant vs. recipient cardiomyocytes.

* $p<0.01$ vs. 4 weeks and recipient cardiomyocytes.

A plasmid encoding reporter genes and cardiac specific gene promoters was used in a previous study to isolate cardiomyocytes from ES cells or embryonic carcinoma cells (EC cell) [21]. Klug et al. [8] transfected a fusion gene containing the α-myosin heavy chain (α-MHC) promoter and aminoglycoside phosphotransferase (NeoR) into pluripotent ES cells, then differentiated these cells in vitro prior to G418 selection. They reported high purification (>99%) and a survival period in the recipient heart of at least 7 weeks following transplantation. Zweigerdt et al. [22] and Zandstra et al. [23] reported a lab-scale protocol to generate cultures of highly enrich cardiomyocyte from ES cells transfected with a α-MHC-NeoR containing plasmid, and suggest its application to a larger-scale process for the supply of stem cell based cardiomyocytes. Muller et al. [9] isolated a subpopulation of ventricular-like cardiomyocytes from ES cells by transfecting the EGFP gene under the control of the MLC-2v promoter and cytomegalovirus enhancer. Moore et al. [24] reported that EC cell (P19Cl6)-derived cardiomyocytes could be isolated using an EGFP reporter under the control of 250 bp of the MLC-2v promoter. They enzymatically digested embryoid bodies, then isolated a population of cardiomyocytes (97% pure) using Percoll gradient centrifugation and FACS analysis. Kolossov et al. [25] reported the use of EGFP under the control of the cardiac α-actin promoter to isolate ES cell-derived cardiomyocytes. The present study confirmed the efficiency of this strategy for the isolation and purification of cardiomyocytes from bone-marrow-derived stem cells.

Reinecke and Murry [26] and Zhang et al. [27] highlighted the importance of a quantitative analysis of grafted cardiomyocytes, since a large number of fetal or neonatal cardiomyocytes often display apoptosis within several days of transplantation. They reported that only a small percentage of cardiomyocytes survive in the cryoinjured recipient heart, and that heat shock or adenoviral transfer of constitutive active Akt genes could increase their survival. In comparison, the present study reports a slightly higher survival rate for bone marrow-derived cardiomyocytes. One possible reason is the difference in the experimental models as the present study used a mouse uninjured model and not a rat cryoinjured heart model. Another reason is the small size of our not fully differentiated transplanted cells compared with fetal or neonatal cardiomyocytes. A small size may allow transplanted cells to go deep into the recipient heart without mechanical injury.

Recently, Takeda et al. [28] reported that the life span of human bone marrow mesenchymal stem cells could be prolonged by infecting the cells with the retrovirus encoding oncogene bmi-1, human papilloma virus E6 and E7, and human telomerase reverse transcriptase over 150 population doublings, and that these cells could be induced to differentiate into cardiomyocyte using 5-azacytidine and co-culture with the rat cardiomyocytes. Although this procedure is not suitable for clinical application at the present stage, the findings provide valuable information on the use of human bone marrow stem cells for the regeneration of cardiomyocytes.

In summary, the present study provides a new model for tissue engineering. Further studies are required to improve cardiomyocyte differentiation and to increase the efficiency of the transplantation procedure.

Acknowledgements

This study was supported in part by the research grants (10B-1) of "Nervous and Mental Disorders from the Ministry of Health and Welfare", Japan, the research grants from the Ministry of Education, Science and Culture, Japan, and the research grants from Health Science Research Grants for Advanced Medical Technology from the Ministry of Welfare, Japan.

References

[1] Leor J, Patterson M, Quinones MJ, Kedes LH, Kloner RA. Transplantation of fetal myocardial tissue into the infarcted myocardium of rat A potential method for repair of infarcted myocardium? Circulation 1996;94(Suppl. 9):II332–6.
[2] Matsushita T, Oyamada M, Kurata H, Masuda S, Takahashi A, Emmoto T, et al. Formation of cell junctions between grafted and host cardiomyocytes at the border zone of rat myocardial infarction. Circulation 1999;100(Suppl. 19):II262–8.
[3] Sakai T, Li RK, Weisel RD, Mickle DA, Kim EJ, Tomita S, et al. Autologous heart cell transplantation improves cardiac function after myocardial injury. Ann Thorac Surg 1999;68:2074–80.
[4] Weissman IL. Translating stem and progenitor cell biology to the clinic: barriers and opportunities. Science 2000;287:1442–6.
[5] Weissman IL, Anderson DJ, Gage F. Stem and progenitor cells: origins, phenotypes, lineage commitments, and transdifferentiations. Annu Rev Cell Dev Biol 2001;17:387–403.
[6] Makino S, Fukuda K, Miyoshi S, Konishi F, Kodama H, Pan J, et al. Cardiomyocytes can be generated from marrow stromal cells in vitro. J Clin Invest 1999;03:697–705.
[7] Hakuno D, Fukuda K, Makino S, Konishi F, Tomita Y, Manabe T, et al. Bone marrow-derived cardiomyocytes (CMG cell) expressed functionally active adrenergic and muscarinic receptors. Circulation 2002;105:380–6.
[8] Klug MG, Soonpaa MH, Koh GY, Field LJ. Genetically selected cardiomyocytes from differentiating embryonic stem cells form stable intracardiac grafts. J Clin Invest 1996;98:216–24.
[9] Muller M, Fleischmann BK, Selbert S, Ji GJ, Endl E, Middeler G, et al. Selection of ventricular-like cardiomyocytes from ES cells in vitro. FASEB J 2000;14:2540–8.
[10] O'Brien TX, Lee KJ, Chien KR. Positional specification of ventricular myosin light chain 2 expression in the primitive murine heart tube. Proc Natl Acad Sci U S A 1993;90:5157–61.
[11] Henderson SA, Spencer M, Sen A, Kumar C, Siddiqui MA, Chien KR. Structure, organization, and expression of the rat cardiac myosin light chain-2 gene. Identification of a 250-base pair fragment which confers cardiac-specific expression. J Biol Chem 1989;264:18142–8.
[12] Kanegae Y, Makimura M, Saito I. A simple and efficient method for purification of infectious recombinant adenovirus. Jpn J Med Sci Biol 1995;47:157–66.
[13] Niwa H, Yamamura K, Miyazaki J. Efficient selection for high-expression transfectants by a novel eukaryotic vector. Gene 1991;108:193–200.

[14] Fukuda K, Izumo S. Angiotensin II potentiates DNA synthesis in AT-1 transformed cardiomyocytes. J Mol Cell Cardiol 1998;30: 2069–80.
[15] Myer A, Olson EN, Klein WH. MyoD cannot compensate for the absence of myogenin during skeletal muscle differentiation in murine embryonic stem cells. Dev Biol 2001;229:340–50.
[16] Yamada H, Akishita M, Ito M, Tamura K, Daviet L, Lehtonen JY, et al. AT2 receptor and vascular smooth muscle cell differentiation in vascular development. Hypertension 1999;33:1414–9.
[17] Jackson KA, Snyder DS, Goodell MA. Skeletal muscle fiber-specific green autofluorescence: potential for stem cell engraftment artifacts. Stem Cells 2004;22:180–7.
[18] Tomita S, Li RK, Weisel RD, Mickle DA, Kim EJ, Sakai T, et al. Autologous transplantation of bone marrow cells improves damaged heart function. Circulation 1999;100(Suppl. 19):II247.
[19] Jackson KA, Majka SM, Wang H, Pocius J, Hartley CJ, Majesky MW, et al. Regeneration of ischemic cardiac muscle and vascular endothelium by adult stem cells. J Clin Invest 2001;107:1395–402.
[20] Condorelli G, Borello U, De Angelis L, Latronico M, Sirabella D, Coletta M, et al. Cardiomyocytes induce endothelial cells to trans-differentiate into cardiac muscle: Implications for myocardium regeneration. Proc Natl Acad Sci U S A 2001;98:10733–8.
[21] Sachinidis A, Fleischmann BK, Kolossov E, Wartenberg M, Sauer H, Hescheler J. Cardiac specific differentiation of mouse embryonic stem cells. Cardiovasc Res 2003;58:278–91.
[22] Zweigerdt R, Burg M, Willbold E, Abts H, Ruediger M. Generation of confluent cardiomyocyte monolayers derived from embryonic stem cells in suspension: a cell source for new therapies and screening strategies. Cytotherapy 2003;5:399–413.
[23] Zandstra PW, Bauwens C, Yin T, Liu Q, Schiller H, Zweigerdt R, et al. Scalable production of embryonic stem cell-derived cardiomyocytes. Tissue Eng 2003;9:767–78.
[24] Moore JC, Spijker R, Martens AC, de Boer T, Rook MB, van der Heyden MA, et al. A P19Cl6 EGFP reporter line to quantify cardiomyocyte differentiation of stem cells. Int J Dev Biol 2004;48:47–55.
[25] Kolossov E, Fleischmann BK, Liu Q, Bloch W, Viatchenko-Karpinski S, Manzke O, et al. Functional characteristics of ES cell-derived cardiac precursor cells identified by tissue-specific expression of the green fluorescent protein. J Cell Biol 1998;143:2045–56.
[26] Reinecke H, Murry CE. Taking the death toll after cardiomyocyte grafting: a reminder of the importance of quantitative biology. J Mol Cell Cardiol 2002;34:251–3.
[27] Zhang M, Methot D, Poppa V, Fujio Y, Walsh K, Murry CE. Cardiomyocyte grafting for cardiac repair: graft cell death and anti-death strategies. J Mol Cell Cardiol 2001;33:907–21.
[28] Takeda Y, Mori T, Imabayashi H, Kiyono T, Gojo S, Miyoshi S, et al. Can the life span of human marrow stromal cells be prolonged by bmi-1, E6, E7, and/or telomerase without affecting cardiomyogenic differentiation? J Gene Med 2004;6:833–45.

Journal of the American College of Cardiology
© 2005 by the American College of Cardiology Foundation
Published by Elsevier Inc.

Vol. 45, No. 4, 2005
ISSN 0735-1097/05/$30.00
doi:10.1016/j.jacc.2004.10.053

PRECLINICAL RESEARCH

Beneficial Effect of Hydroxyfasudil, a Specific Rho-Kinase Inhibitor, on Ischemia/Reperfusion Injury in Canine Coronary Microcirculation In Vivo

Toyotaka Yada, MD, PHD,* Hiroaki Shimokawa, MD, PHD,† Osamu Hiramatsu, PHD,* Tatsuya Kajita, MD, PHD,* Fumiyuki Shigeto, MD, PHD,* Etsuro Tanaka, MD, PHD,‡ Yoshiro Shinozaki, BS,§ Hidezo Mori, MD, PHD,‖ Takahiko Kiyooka, MD,# Masashi Katsura, PHD,¶ Seitaro Ohkuma, MD, PHD,¶ Masami Goto, MD, PHD,* Yasuo Ogasawara, PHD,* Fumihiko Kajiya, MD, PHD#

Kurashiki, Fukuoka, Tokyo, Isehara, Suita, and Okayama, Japan

OBJECTIVES We examined whether hydroxyfasudil, a specific Rho-kinase inhibitor, exerts cardioprotective effect on coronary ischemia/reperfusion (I/R) injury and, if so, whether nitric oxide (NO) is involved.

BACKGROUND Recent studies have demonstrated that Rho-kinase is substantially involved in the pathogenesis of cardiovascular diseases; however, it remains to be examined whether it is also involved in ischemia/reperfusion (I/R) injury.

METHODS Canine subepicardial small arteries (SA, ≥100 μm) and arterioles (A, <100 μm) were observed by a charge-coupled device intravital microscope during I/R. Coronary vascular responses to endothelium-dependent (acetylcholine, intracoronary [IC]) and -independent (papaverine, IC) vasodilators were examined after I/R under the following four conditions: control (n = 7), NO synthase inhibitor alone (N^G-monomethl-L-arginine [L-NMMA], IC, n = 4), hydroxyfasudil alone (IC, n = 7), and hydroxyfasudil plus L-NMMA (n = 7).

RESULTS Hydroxyfasudil significantly attenuated serotonin (IC)-induced vasoconstriction of SA (−7 ± 1% vs. 2 ± 1%, $p < 0.01$). Coronary I/R significantly impaired coronary vasodilation to acetylcholine after I/R (SA, $p < 0.05$; and A, $p < 0.01$ vs. before I/R) and L-NMMA further reduced the vasodilation, whereas hydroxyfasudil completely preserved the responses. The vasoconstriction by L-NMMA after I/R was significantly improved by hydroxyfasudil in both-sized arteries (both $p < 0.01$). Expression of endothelial nitric oxide synthase (eNOS) protein in the ischemic endocardium of left anterior descending coronary artery area (as determined by Western blotting) significantly decreased (79 ± 4%) compared with the nonischemic endocardium of LCX area (100 ± 7%), which was improved by hydroxyfasudil (105 ± 6%, $p < 0.01$). Hydroxyfasudil significantly reduced myocardial infarct size, and hydroxyfasudil with L-NMMA also reduced the infarct size compared with L-NMMA alone.

CONCLUSIONS Hydroxyfasudil exerts cardioprotective effects on coronary I/R injury in vivo, in which NO-mediated mechanism may be involved through preservation of eNOS expression. (J Am Coll Cardiol 2005;45:599–607) © 2005 by the American College of Cardiology Foundation

Ischemia-reperfusion (I/R) injury attenuates endothelium-dependent dilation of large coronary arteries both in vitro (1,2) and in vivo (3,4). Endothelial dysfunction causes adverse outcome in the coronary circulation (5). Reperfusion injury is caused by direct myocardial injury through coronary vasospasm, free radicals, and inflammatory responses (6,7). Furthermore, local coronary vasoconstrictions in response to vasoconstrictors (e.g., serotonin) are enhanced (8,9). However, the mechanism of I/R-induced vascular injury remains to be clarified.

Recent studies have demonstrated that Rho-kinase, an effector of the small guanosine triphosphatase Rho, is substantially involved in the pathogenesis of cardiovascular diseases (10). Shimokawa et al. (10,11) have recently found that hydroxyfasudil is a potent and specific inhibitor of Rho-kinase and markedly inhibits coronary hyperconstriction and macrophage migration. They also demonstrated that intracoronary serotonin induces coronary hypercontractions at the inflammatory coronary lesions both in vitro and in vivo, in which up-regulated Rho-kinase is substantially

From the *Department of Medical Engineering and Systems Cardiology, Kawasaki Medical School, Kurashiki, Japan; †Department of Cardiovascular Medicine, Kyushu University Graduate School of Medical Sciences, Fukuoka, Japan; ‡Faculty of Applied Bioscience, Tokyo University of Agriculture, Tokyo, Japan; §Department of Physiology, Tokai University School of Medicine, Isehara, Japan; ‖Department of Cardiac Physiology, National Cardiovascular Center Research Institute, Suita, Japan; ¶Department of Pharmacology, Kawasaki Medical School, Kurashiki, Japan; and #Department of Cardiovascular Physiology, Okayama University Graduate School of Medicine and Dentistry, Okayama, Japan. This work was supported in part by grants from the Japanese Ministry of Education, Science, Sports, Culture, and Technology, Tokyo, Japan (Nos. 13307024, 13557068, 14657178, and 16300164); and the Program for Promotion of Fundamental Studies in Health Sciences of the Organization for Pharmaceutical Safety and Research of Japan.

Manuscript received September 2, 2004; revised manuscript received October 1, 2004, accepted October 18, 2004.

JACC Vol. 45, No. 4, 2005
February 15, 2005:599–607

Abbreviations and Acronyms
I/R = ischemia-reperfusion
LAD = left anterior descending coronary artery
LCX = left circumflex artery
NO = nitric oxide

involved (12). Recent studies demonstrated that endothelial expression and activity of Rho-kinase are enhanced by hypoxia, with a resultant down-regulation of endothelial nitric oxide synthase (eNOS) expression and reduced nitric oxide (NO) production (13), and that Rho-kinase is also involved in a canine model of cerebral infarction associated with superoxide production and neutrophil infiltration (14).

It is conceivable that Rho-kinase is involved in the mechanisms of I/R injury associated with reduced endothelial NO production. In this study, we thus examined whether hydroxyfasudil exerts protective effect on coronary I/R injury in vivo and, if so, whether NO is involved.

METHODS

Animal preparation. This study conformed to the Guideline on Animal Experiments of Kawasaki Medical School and the Guide for the Care and Use of Laboratory Animals published by the U.S. National Institutes of Health.

Mongrel dogs (15 to 25 kg, n = 31) of either gender were anesthetized with morphine (3 mg/kg, intramuscular) and sodium pentobarbital (25 mg/kg, intravenous). After intubation, each animal was ventilated with a high-frequency jet ventilator (model VS600, IDC, Pittsburgh, Pennsylvania) with room air supplemented by 100% oxygen. Aortic pressure and left ventricular pressure were continuously monitored with an 8-F pigtail double manometer catheter (SPC-784A, Millar, Texas). The proximal portion of the left anterior descending coronary artery (LAD) was isolated and a transonic flow probe (T206, Transonic Systems, Ithaca, New York) was placed around the vessel.

Needle-probe intravital microscope. The needle-probe (4.5 mm in diameter, VMS 1210, Nihon Kohden, Tokyo, Japan) contains a gradient index lens (with a magnification of 200) surrounded by light guide fibers and a double lumen sheath. A doughnut-shaped balloon on the tip avoids direct compression of the vessels by the needle tip (15).

Measurements of coronary diameters. We placed the needle probe gently on subepicardial microvessels. When a clear vascular image was obtained, end-diastolic vascular images were taken with 30 pictures/s (15).

Measurements of regional myocardial blood flow. Regional myocardial blood flow was determined by the nonradioactive microsphere (Sekisui Plastic Co, Ltd, Tokyo, Japan) technique, as previously described in detail (16). Briefly, 1 ml of the microspheres suspension (2 to 4 $\times$ 10^6 spheres) was injected into the left atrium 85 min after the onset of coronary occlusion. Just before microsphere administration, a reference blood flow sample was drawn from the femoral artery at a constant rate of 8 ml/min for 2 min. The X-ray fluorescence of the stable heavy elements was measured by a wavelength-dispersive spectrometer (model PW 1480, Phillips Co., Ltd., Eindhoven, the Netherlands) (16). Myocardial blood flow was calculated according to the formula: time flow = tissue counts $\times$ (reference flow/reference counts) and was expressed in ml/g per minute (16).

Western blotting. Proteins were separated on sodium dodecyl sulfate (SDS)/polyacrylamide gel electrophoresis as previously described (17). The tissues were homogenized in a sample buffer (100 mM Tris-HCl [pH 6.8], 4% SDS, 0.2% glycerol). The tissue lysate was centrifuged and the supernatant collected. Protein concentration was quantified by a bicinchoninate (BCA) protein assay kit (Pierce Chemical, Rockford, Illinois). An aliquot of 10 μg of protein from each sample was electrophoresed on a 7.5% SDS-polyacrylamide gel. Proteins were subsequently transferred to polyvinylidine difluoride membrane (Immobilon-P membrane, Millipore, Bedford, Massachusetts) electrophoretically (100 V for 1 h) and membranes were incubated with antibody. The antibodies used in this study were rabbit anti-phosphorylated ezrin/radixin/moesin (ERM) family, total ERM. The antibody against phosphorylated ERM recognizes human moesin (phosphorylated at Thr558), which also binds to the phosphorylated ezrin (Thr567) and radixin (Thr564). Therefore, we used the extent of phosphorylation of ERM as a marker of Rho-kinase activity. The levels of Western blot for phosphorylated ERM were normalized to those for total ERM as a control. Membranes were then incubated with a horseradish peroxidase-conjugated horse anti-rabbit immunoglobulin G antibody (1:5,000). Immunoreactivity was detected by enhanced chemiluminescence autoradiography (ECL Western blotting detection kit; Amersham Pharmacia Biotechnology, United Kingdom).

The obtained samples were washed with ice-cold Tris-HCl buffer (pH 7.4), mixed with the sample buffer (4% sodium lauryl sulfate, 12% beta-mercaptoethanol, and 20% glycerol in 100 mM Tris-HCl [pH 6.8]), sonicated (1 min), boiled (3 min), and finally centrifuged (10,000 g, 60 min, 4°C). The resultant supernatant was stored at −80°C until use. The separation of proteins was carried out according to the previous study (18), with a minor modification. The relative intensity of immunoreactive bands was quantified by Image Master 1D Elite software (Amersham Biotech, Buckinghamshire, United Kingdom), and the data were estimated as percentage of each control.

Experimental protocols. After the surgical procedure and instrumentation, at least 30 min were allowed for stabilization while hemodynamic variables were monitored. The following protocols were examined.

1. We infused graded doses of hydroxyfasudil (10, 30, and 100 μg/kg, IC), and coronary vascular responses were

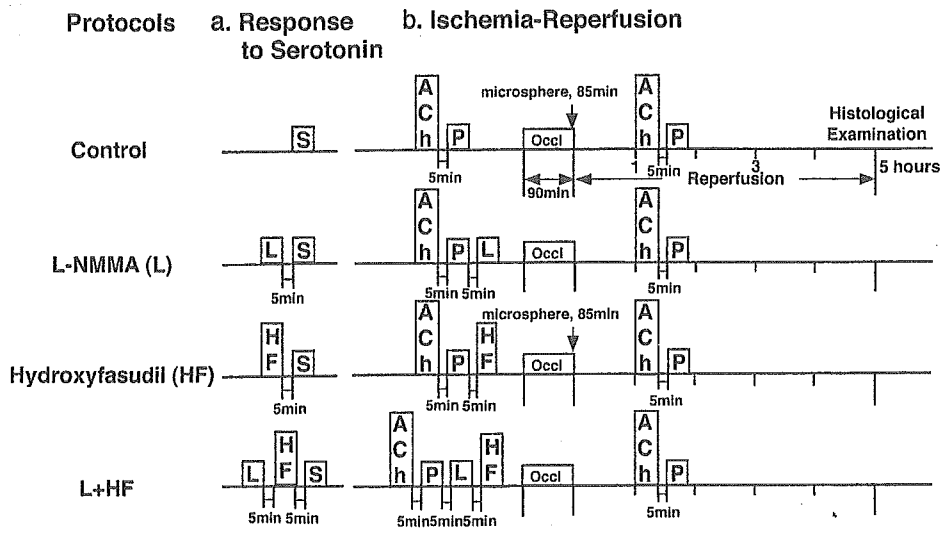

Figure 1. Experimental protocol. S = serotonin; L = L-NMMA; HF = hydroxyfasudil; Ach = acetylcholine; P = papaverine; Occl = coronary occlusion.

analyzed for 4 min by measuring end-diastolic vascular diameters and flows of the LAD.

2. The arteriolar vasoconstrictor response to serotonin before and after hydroxyfasudil (100 μg/kg, IC) was examined with or without inhibition of NO synthase (L-NMMA, 2 μmol/min for 20 min, IC) (Fig. 1). Hydroxyfasudil or L-NMMA was administered at 5 min before infusion of serotonin. The time interval between L-NMMA and hydroxyfasudil was also 5 min.
3. The arteriolar vasodilator responses to endothelium-dependent (acetylcholine, 1 μg/kg IC) and -independent (papaverine, 1 mg IC) vasodilators were examined before and after coronary I (90 min)/R (60 min) under the following four conditions separately in different animals: 1) control conditions, 2) L-NMMA alone, 3) hydroxyfasudil alone (100 μg/kg IC), and 4) hydroxyfasudil plus L-NMMA (Fig. 1). The time interval between each treatment was also 5 min. The basal coronary diameter is before administration of acetylcholine or papaverine either before or after I/R. Hydroxyfasudil and L-NMMA were administered at 5 min after administration of acetylcholine or papaverine. Microspheres were administered at 85 min after the onset of coronary occlusion.
4. After 5 h of reperfusion, LAD and the left circumflex artery (LCX) and myocardial tissue of LAD and LCX area were obtained for Western blotting. We reoccluded the LAD and injected Evans blue dye into a systemic vein. Then myocardial slices (5 mm) were incubated in 1% 2,3,5-triphenyltetrazolium chloride (Sigma, Japan) solution to detect the infarct area. Infarct size was expressed as percentage of the infarct area that was contiguous with area at risk (19).

Drugs. We used the following drugs: hydroxyfasudil (Asahi Kasei Pharma, Tokyo, Japan), acetylcholine (Daiichi-Seiyaku, Tokyo, Japan), papaverine (Dainihon-Seiyaku, Tokyo, Japan), and N^G-methyl-L-arginine (L-

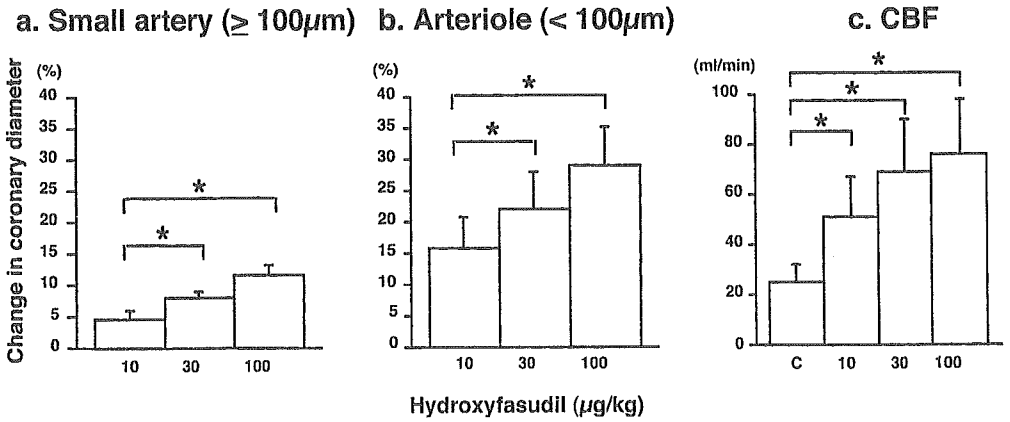

Figure 2. Coronary vasodilator effects of hydroxyfasudil in dogs in vivo. Hydroxyfasudil (10, 30, and 100 μg/kg, IC) caused coronary vasodilation, in a dose-dependent manner, under normal conditions in both small arteries **(a)** and arterioles **(b)**. Number of vessels per animal used was 5/3 in small arteries and 7/4 in arterioles, respectively. Hydroxyfasudil also increased coronary blood flow (CBF) in a dose-dependent manner **(c)**. *$p < 0.05$.

JACC Vol. 45, No. 4, 2005
February 15, 2005:599–607

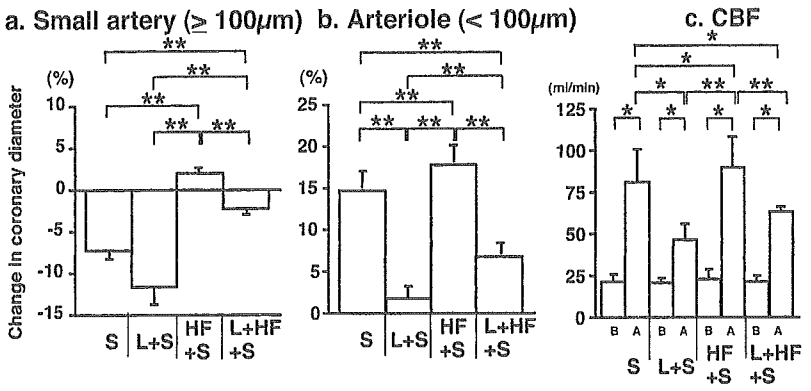

Figure 3. Effects of hydroxyfasudil on serotonin-induced coronary vascular responses in dogs in vivo. Hydroxyfasudil converted the serotonin-induced vasoconstriction of small arteries to vasodilation **(a)** and significantly enhanced the serotonin-induced vasodilation of arterioles **(b)**. L-NMMA significantly attenuated the serotonin-induced vasodilation, which was counteracted by hydroxyfasudil. Number of vessels per animal used was 18/6 for S, L + S and HF + S, 13/4 for L + HF + S. *$p < 0.05$, **$p < 0.01$. S = serotonin; L = L-NMMA; HF = hydroxyfasudil; B = before drug; A = after drug.

NMMA, Sigma). All drugs were diluted in a physiologic saline immediately before use.

Statistical analysis. Results are expressed as means ± SEM. Vascular responses (Figs. 2a to 2c, 3c, 4c, 6c, 7a to 7c, 8a) were analyzed by one-way analysis of variance followed by Scheffe's post-hoc test for multiple comparisons. Difference in the effects of serotonin, acetylcholine, and papaverine on subepicardial microvessels before and after I/R (Figs. 3a, 3b, 4a, 4b, 5a to 5d, 6a, and 6b), and difference between infarct size/risk area and transmural collateral flow with or without hydroxyfasudil (Fig. 8b) were examined by a multiple regression analysis using a model in which the change in coronary diameter was set as a dependent variable (y) and vascular size as an explanatory variable (x) while the statuses of hydroxyfasudil and hydroxyfasudil plus L-NMMA were set as dummy variables (D_1, D_2) in the following equation; $y = a_0 + a_1x + a_2D_1 + a_3D_2$, where a_0 through a_3 are partial regression coefficients. The criterion for statistical significance was at $p < 0.05$.

RESULTS

Coronary vasodilator effects of hydroxyfasudil. Intracoronary administration of hydroxyfasudil caused a significant coronary vasodilation of both small arteries and arterioles (Figs. 2a and 2b, both $p < 0.05$, 10 μg/kg vs. 30 and 100 μg/kg) in a dose-dependent manner under control conditions with a resultant increase in CBF (Fig. 2c, $p < 0.05$, C vs. 10, 30 and 100 μg/kg). Intracoronary hydroxyfasudil did not significantly alter mean aortic pressure or heart rate (Table 1).

Hemodynamics and blood gases during I/R injury. In each experimental condition, mean aortic pressure and heart rate at baseline were constant and comparable (Table 1), and oxygen partial pressure (P_{O_2}), carbon dioxide partial pressure (P_{CO_2}), and pH were maintained within the physiologic ranges (pH 7.35 to 7.45, P_{CO_2} 25 to 40 mm Hg, P_{O_2} >70 mm Hg) throughout the experiments. Hemodynamic

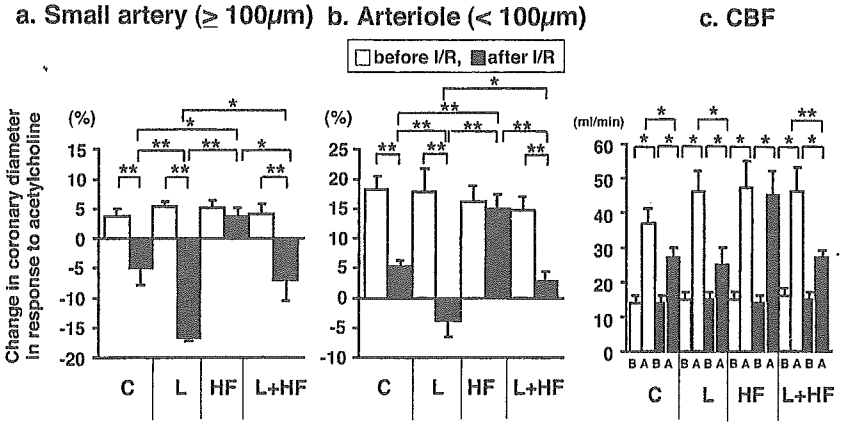

Figure 4. Endothelium-dependent coronary vasodilation before and after coronary ischemia/reperfusion (I/R) injury in dogs in vivo. Coronary I/R significantly impaired coronary vasodilation to acetylcholine under control conditions (C) and L-NMMA (L) further suppressed the vasodilation, whereas hydroxyfasudil (HF) completely preserved the responses. The vasoconstriction induced by L-NMMA after I/R was significantly improved by hydroxyfasudil in small arteries. Hydroxyfasudil also prevented the decrease in coronary blood flow (CBF) after I/R, which effect was attenuated by L-NMMA. Number of vessels per animals used was 7/6 for control (mean diameter 120 ± 7 μm), 5/4 for L-NMMA (123 ± 8 μm), 6/4 for hydroxyfasudil (118 ± 8 μm), and 5/4 for hydroxyfasudil plus L-NMMA (125 ± 9 μm) in small arteries, and 12/6 for control (70 ± 6 μm), 8/4 for L-NMMA (69 ± 7 μm), 8/5 for hydroxyfasudil (68 ± 7 μm), and 11/6 for hydroxyfasudil plus L-NMMA (71 ± 5 μm) in arterioles. I/R = ischemia/reperfusion; B = before acetylcholine; A = after acetylcholine. *$p < 0.05$; **$p < 0.01$.

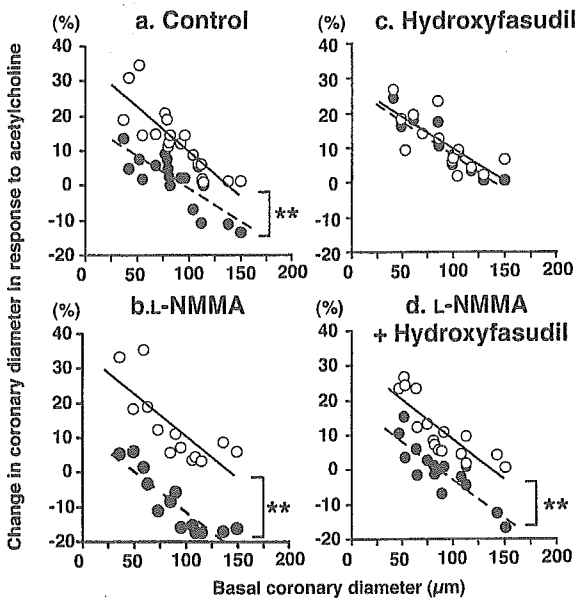

Figure 5. Coronary microvascular responses to acetylcholine before and after coronary ischemia/reperfusion (I/R) injury in dogs in vivo. Under control conditions, I/R significantly impaired coronary vasodilator response to acetylcholine **(a)**, whereas hydroxyfasudil completely preserved the responses in the absence **(c)** or presence of L-NMMA **(d)** compared with that in the presence of L-NMMA alone **(b)**. Number of vessels per animals used was 19/7 under control conditions (before I/R: $y = -0.3x + 35.9$, $r = 0.85$; after I/R: $y = -0.2x + 18.1$, $r = 0.80$), 13/4 for L-NMMA alone (before I/R: $y = -0.2x + 35.1$, $r = 0.76$; after I/R: $y = -0.2x + 12.2$, $r = 0.88$), 14/7 for hydroxyfasudil (before I/R: $y = -0.2x + 27.9$, $r = 0.73$; after I/R: $y = -0.2x + 27.4$, $r = 0.80$), and 16/7 for hydroxyfasudil plus L-NMMA (before I/R: $y = -0.2x + 31.8$, $r = 0.83$; after I/R: $y = -0.2x + 19.2$, $r = 0.86$). **$p < 0.01$. **Open circles** = before I/R; **solid circles** = after I/R.

variables at baseline did not significantly change after I/R compared with those before I/R (Table 1).

Effects of Rho-kinase inhibition on serotonin-induced coronary responses. Intracoronary administration of serotonin caused coronary vasoconstriction of small arteries and vasodilation of arterioles under control conditions (Figs. 3a and 3b, both $p < 0.01$ vs. basal coronary diameter). Intracoronary administration of L-NMMA enhanced the serotonin-induced vasoconstriction and abolished the serotonin-induced vasodilation of arterioles (Fig. 3b, $p < 0.01$ vs. serotonin, S). By contrast, hydroxyfasudil reversed the serotonin-induced vasoconstriction of small arteries to vasodilation while it further enhanced the serotonin-induced vasodilation of arterioles (Figs. 3a and 3b, both $p < 0.01$). The vasodilator effect of hydroxyfasudil on the coronary response to serotonin was significantly attenuated by L-NMMA in both-sized arteries (Figs. 3a and 3b, both $p < 0.01$). As a result, serotonin-induced increase in CBF (Fig. 3c) was significantly inhibited by L-NMMA ($p < 0.05$) and enhanced by hydroxyfasudil ($p < 0.05$), the effect of which was significantly attenuated by L-NMMA ($p < 0.01$).

Endothelium-dependent coronary vasodilation before and after I/R. Under control conditions (before I/R), intracoronary administration of acetylcholine caused a significant coronary vasodilation to a greater extent in arterioles than in small arteries (Figs. 4a, 4b, and 5a, $p < 0.01$). Coronary I/R significantly impaired the coronary vasodilation to acetylcholine in both sized arteries (both $p < 0.01$) and L-NMMA further reduced the vasodilation (Figs. 4a, 4b, and 5b both $p < 0.01$), whereas hydroxyfasudil completely preserved (small artery $p < 0.05$, arteriole $p < 0.01$) the acetylcholine-induced coronary vasodilator response after I/R (Figs. 4a and 4b). The vasoconstriction by L-NMMA was significantly attenuated by hydroxyfasudil in both sized arteries (both $p < 0.05$) with decrement of CBF (Figs. 4a to 4c). When the coronary vasodilator response to acetylcholine was expressed as a function of basal coronary diameter, hydroxyfasudil preserved the response after I/R injury at all sized coronary arteries either in the absence

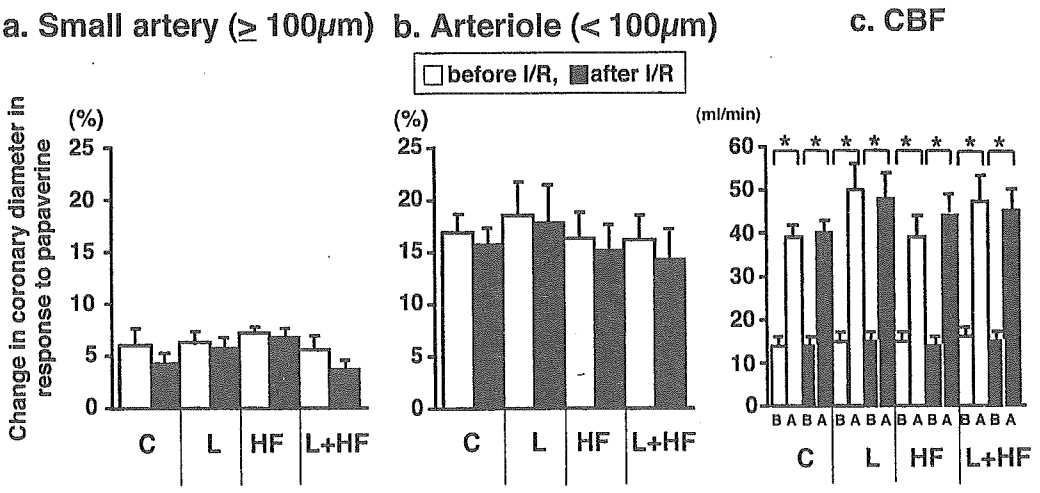

Figure 6. Endothelium-independent coronary vasodilation before and after coronary I/R injury in dogs in vivo. Coronary vasodilator response to papaverine was comparable under all conditions in both small arteries and arterioles. Number of vessels per animals used was 7/6 for control (mean diameter 120 ± 7 μm), 5/4 for L-NMMA (123 ± 8 μm), 6/4 for hydroxyfasudil (118 ± 8 μm), and 5/4 for hydroxyfasudil plus L-NMMA (125 ± 9 μm) in small arteries; and 12/6 for control (70 ± 6 μm), 8/4 for L-NMMA (69 ± 7 μm), 8/5 for hydroxyfasudil (68 ± 7 μm), and 11/6 for hydroxyfasudil plus L-NMMA (71 ± 5 μm) in arterioles. C = control; L = L-NMMA; HF = hydroxyfasudil. I/R = ischemia/reperfusion. B = before papaverine; A = after papaverine.

JACC Vol. 45, No. 4, 2005
February 15, 2005:599–607

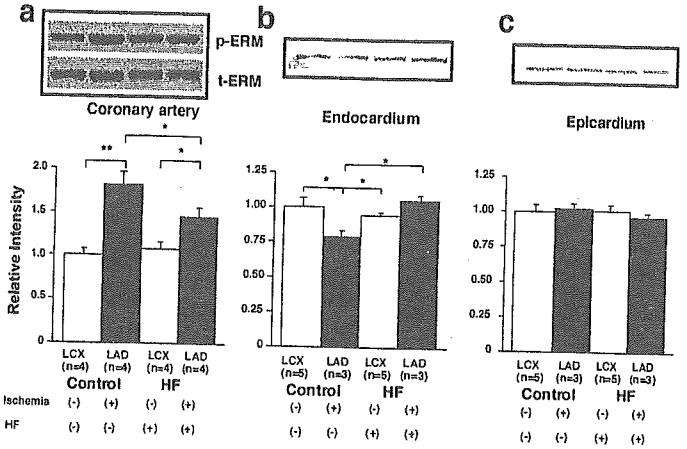

Figure 7. Western blotting showing the effects of hydroxyfasudil (HF) on Rho-kinase activity and on eNOS protein expression in the myocardium of LAD and LCX. **(a)** Rho-kinase activity in coronary artery; **(b)** expression of eNOS protein in endocardium; **(c)** expression of eNOS protein in epicardium. Rho-kinase activity was determined by the degree of ezrin-radixin-moesin phosphorylation (p-ERM/t-ERM). Rho-kinase activation in the ischemic LAD was completely inhibited by cotreatment with hydroxyfasudil. Expression of eNOS protein in the ischemic endocardium of LAD area was significantly decreased compared with the non-ischemic endocardium of LCX area, which was again improved by hydroxyfasudil. $^{*}p < 0.05$, $^{**}p < 0.01$.

(Figs. 4a, 4b, and 5c, df 2, 25, $p < 0.01$) or presence (Figs. 4a, 4b, and 5d, df 2, 24, $p < 0.01$) of L-NMMA compared with that in the presence of L-NMMA alone (Figs. 4a, 4b, and 5b).

Endothelium-independent coronary vasodilation. Coronary vasodilator response to papaverine was comparable under all conditions in both small arteries and arterioles (Figs. 6a and 6b). Similarly, the increase in CBF to papaverine (Fig. 6c) was also comparable under all conditions in both-sized arteries. Those coronary vasodilator responses were resistant to the blockade of NO synthesis with L-NMMA (Figs. 6a and 6b).

Activation of Rho-kinase by ischemia-reperfusion causes down-regulation of eNOS protein expression. Rho-kinase activity after a 90-min period of ischemia was significantly greater in the ischemic LAD than in the nonischemic LCX in the control group (Fig. 7a, $p < 0.01$). This Rho-kinase activation was significantly suppressed by hydroxyfasudil in the ischemic LAD (Fig. 7a, $p < 0.01$). Expression of eNOS protein in the ischemic endocardium of the LAD area (as determined by Western blotting) was significantly decreased (79 ± 4%, $p < 0.05$) compared with the nonischemic endocardium of the LCX area (100 ± 7%), which was also improved by hydroxyfasudil (105 ± 6%) (Fig. 7b, $p < 0.05$). There was no significant difference in the eNOS expression in the epicardium between the LAD and LCX area (Fig. 7c).

Effect of Rho-kinase inhibition on I/R-induced myocardial infarct size. Ischemia-reperfusion injury caused myocardial infarct area that was approximately 50% of the left ventricular risk area, and intracoronary L-NMMA did not further increase the I/R-induced infarction size (Fig. 8a). Intracoronary pretreatment with hydroxyfasudil markedly reduced the infarct size ($p < 0.01$ vs. control), and this beneficial effect of hydroxyfasudil was significantly attenuated by L-NMMA (Fig. 8a $p < 0.01$). In the control group, there was an inverse relation between the infarct area and collateral blood flow measured by microsphere technique ($r = 0.93$, $p < 0.01$), and hydroxyfasudil significantly shifted the regression line downward as compared with the control group ($p < 0.01$), that is, smaller infarct size for a given collateral flow (Fig. 8b).

DISCUSSION

The major findings of the present in vivo study in the canine coronary microcirculation were that: 1) a specific Rho-kinase inhibitor hydroxyfasudil preserved the endothelium-dependent coronary vasodilator responses after coronary I/R injury, 2) hydroxyfasudil also reduced myocardial infarct size, and 3) NO may be involved in those cardiovascular protective effects of hydroxyfasudil. To the best of our knowledge, this is the first report that demonstrates the usefulness of a Rho-kinase inhibitor to prevent coronary I/R injury in vivo.

Validations of experimental model and methodology. On the basis of the previous reports (4,12,20), we chose the adequate dose of hydroxyfasudil, acetylcholine, papaverine, and L-NMMA to examine the effects of the Rho-kinase inhibition, endothelium-dependent and -independent vasodilator responses, and inhibition of NO synthesis on coronary vascular responses before and after coronary I/R, respectively. The methodologic validity of the present study has been confirmed previously (15). After 60 to 90 min of ischemia, ultrastructural damage of coronary endothelium was observed particularly in the subendocardium in the present study, a consistent finding to the previous study (21).

Hydroxyfasudil as a specific Rho-kinase inhibitor in the coronary microcirculation in vivo. Shimokawa et al. (11) have recently demonstrated that hydroxyfasudil is a specific Rho-kinase inhibitor that markedly inhibits coronary vasospastic responses in a porcine model; its inhibitory effect on Rho-kinase is 100 times greater than on protein kinase C and

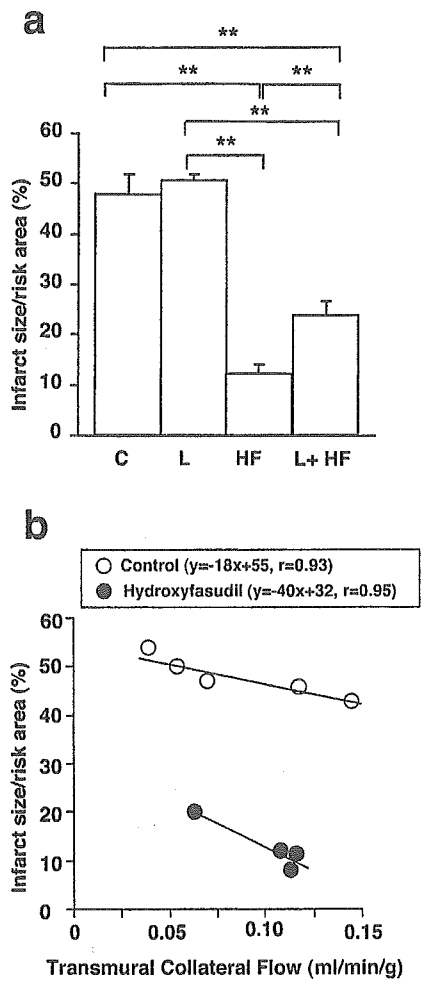

Figure 8. **(a)** Ischemia/reperfusion (I/R)-induced LV infarct size in dogs in vivo. Hydroxyfasudil significantly reduced the I/R-induced LV infarct size. The beneficial effect of hydroxyfasudil was partially attenuated by L-NMMA, while L-NMMA alone did not significantly increase the infarct size. Number of animals used was each 7 for C, HF, and L + HF, and 4 for L. C = control; L = L-NMMA; HF = hydroxyfasudil. **$p < 0.01$. **(b)** Plot of infarct size expressed as a percentage of the risk area and regional collateral flow during ischemia. In the control group, there was an inverse relation between infarct area and collateral flow measured by microsphere ($r = 0.93$, $p < 0.01$), and hydroxyfasudil significantly shifted the regression line downward as compared with the control group ($p < 0.01$). Number of animals used was five for control conditions and four for hydroxyfasudil.

1,000 times greater on myosin light-chain kinase. Hydroxyfasudil has potent vasodilator effects on coronary arteries through inhibition of Rho-kinase-mediated phosphorylations of myosin light chains (11). In the present study, intracoronary hydroxyfasudil caused coronary microvascular vasodilation in a dose-dependent manner in vivo, and its vasodilator effect was greater in arterioles than in small arteries (Fig. 2). Hydroxyfasudil suppressed the serotonin-induced vasoconstriction of small arteries, whereas it enhanced the serotonin-induced vasodilation of arterioles in vivo (Fig. 3). This finding is in accordance with the hypothesis that the calcium sensitization of vascular smooth-muscle cells mediated by Rho-kinase plays a key role in the molecular mechanisms of coronary hyperconstriction (12). Furthermore, in the present study, intracoronary L-NMMA significantly attenuated serotonin-induced coronary vasodilator responses, which were improved by hydroxyfasudil, indicating an involvement of NO-mediated mechanism in the beneficial effects of the Rho-kinase inhibitor. Lamping et al. (22) demonstrated that coronary vascular response to serotonin is determined by a balance between 5-HT_1 receptor-mediated dilatation of coronary arterioles and 5-HT_2 receptor-mediated vasoconstriction of small coronary arteries. Inhibition of NO synthase enhances coronary vasoconstriction to serotonin in both-sized arteries. Our present results are in agreement with those of Lamping et al. The beneficial vasodilator effect of hydroxyfasudil on coronary vascular response to serotonin is mediated by its action on both vascular smooth muscle and the endothelium as shown in Figure 3. Thus, it is possible that the beneficial effect of Rho-kinase blockade with hydroxyfasudil is mediated by its action on both vascular smooth muscle and the endothelium (22). Serotonin released by aggregating platelets has been implicated for coronary vasospasm in the presence of damaged vascular endothelium (5,23).

Beneficial effects of a Rho-kinase inhibitor on coronary I/R injury. In the present study, hydroxyfasudil exerted beneficial effects on I/R-induced endothelial injury in the canine coronary microcirculation in vivo through the NO-dependent mechanism (Figs. 4 and 5). This dose of hydroxyfasudil (100 μg/kg) selectively inhibits Rho-kinase activity and effectively prevents serotonin-induced coronary hyperconstriction. Recent studies have demonstrated that cGMP-dependent protein kinase inhibits RhoA phosphorylation by inhibiting the membrane binding of RhoA, in which the NO-mediated mechanism may inhibit the RhoA/Rho-kinase pathway (24–26). It was previously demonstrated that statins attenuate I/R injury of the heart and the brain in rats and mice, demonstrating the Rho-mediated and NO-dependent protective effect of statins (27,28). Hydroxyfasudil also inhibits the production of superoxide anions in neutrophils (29) and various chemoattractant-induced migration of those cells (14) in a canine model of cerebral ischemia. Furthermore, treatment with hydroxyfasudil in human saphenous vein endothelial cells reversed the hypoxia-induced decrease in eNOS activity as examined by the citrulline conversion assay and 4,5-diaminofluorescein diacetate fluorescence method (13). In the present study, I/R increased Rho-kinase activity, and hydroxyfasudil significantly inhibited the Rho-kinase activation. These findings suggest that NO is involved in the protective effect of hydroxyfasudil with an increase in eNOS activity and a decrease in Rho-kinase activity during reperfusion injury.

In the present study, the vasodilator effects of hydroxyfasudil were significantly attenuated by L-NMMA (Figs. 3 and 4). The eNOS expression was decreased in the ischemic area of the endocardium compared with that of the epicardium under control conditions, which was improved by hydroxyfasudil (Fig. 7). We have previously demonstrated that endocardial arteriolar dilation during reactive hyperemia is more sensitive to L-NMMA than epicardial arte-

JACC Vol. 45, No. 4, 2005
February 15, 2005:599–607

Table 1. Hemodynamics During Myocardial Ischemia-Reperfusion Injury in Dogs

	n	Before I/R			After I/R		
		Baseline	ACh	Papaverine	Baseline	ACh	Papaverine
MBP (mm Hg)							
Control	7	91 ± 4	90 ± 6	92 ± 5	89 ± 4	89 ± 5	92 ± 6
L-NMMA	4	88 ± 8	86 ± 5	91 ± 7	86 ± 4	86 ± 4	85 ± 4
Hydroxyfasudil	7	92 ± 9	92 ± 8	93 ± 8	93 ± 6	90 ± 6	91 ± 7
L-NMMA + hydroxyfasudil	7	89 ± 6	89 ± 5	89 ± 5	91 ± 8	87 ± 10	89 ± 9
Heart rate (beats/min)							
Control	7	151 ± 5	156 ± 3	155 ± 3	155 ± 5	153 ± 5	152 ± 5
L-NMMA	4	147 ± 7	149 ± 8	149 ± 8	145 ± 11	146 ± 11	145 ± 11
Hydroxyfasudil	7	152 ± 7	151 ± 8	148 ± 8	148 ± 7	149 ± 7	150 ± 7
L-NMMA + hydroxyfasudil	7	151 ± 6	152 ± 6	151 ± 6	154 ± 6	151 ± 6	153 ± 7

Results are expressed as mean ± SEM.
ACh = acetylcholine; I/R = ischemia/reperfusion; MBP = mean blood pressure.

riolar dilation (30). These findings indicate that the perfusion of the endocardium is more dependent on NO than that of the epicardium and that endothelial damage after I/R in arterioles may be greater in the endocardium than in the epicardium.

In the present study, hydroxyfasudil exerted cardiovascular protective effects on coronary I/R injury, as did preconditioning (31,32). However, the mechanism by which hydroxyfasudil and preconditioning protect coronary I/R injury appears to be different. Endogenous NO does not alter the infarct size after I/R and is not involved in the protective mechanism of preconditioning in pigs or rabbits (33,34). It has been suggested that preconditioning preserves myocardial creatine phosphate and intracellular pH (35). Furthermore, ischemic preconditioning increases adenosine production and activates protein kinase C, which also enhances adenosine production during I/R injury.

In the present study, hydroxyfasudil significantly reduced myocardial infarct size with increment of coronary collateral blood flow, at least in part, thorough the NO-mediated mechanism (Fig. 8). Shimokawa et al. (11) demonstrated that hydroxyfasudil inhibits both MLC mono- and diphosphorylations. Satoh et al. (14) showed that hydroxyfasudil also protects the brain from ischemic injury through inhibition of superoxide production and neutrophil infiltration. Mohri et al. (36) demonstrated that fasudil suppresses coronary microvascular spasm in patients with microvascular angina. Wolfrum et al. (37) recently demonstrated that inhibiting Rho-kinase has cardioprotective effects to reduce infarct size by activating phosphatidylinositol 3-kinase/protein kinase Akt/eNOS pathways. All these mechanisms may be involved in the beneficial effects of hydroxyfasudil on the I/R-induced myocardial injury.

Hydroxyfasudil increases blood supply to the ischemic region of the myocardium and prevents I/R-induced myocardial injury. Furthermore, it has been recently demonstrated that an estrogen receptor modulator, raloxifene, also reduces I/R-induced myocardial infarct size, whereas an inhibitor of NO synthesis (L-NAME) or a blocker of calcium-activated K^+ channels (charybdotoxin) partly attenuates the effect of raloxifene (19). These results suggest that cardioprotective effects of those inhibitors may be mediated in part by the compensatory effects of NO and endothelium-derived hyperpolarizing factor (20). Several studies using NO synthase inhibitors (38,39) or eNOS-deficient mice (40) demonstrated an increase in infarct size after I/R. The effect of NO synthesis inhibition on the infarct size might be species- and dose-dependent.

Clinical implications and conclusions. The present study has demonstrated for the first time that hydroxyfasudil, a specific Rho-kinase inhibitor, has NO-dependent cardiovascular protective effects on coronary I/R injury in vivo. Rho-kinase inhibitor has also an antianginal effect in a canine model of angina (41), patients with effort angina (42), and those with vasospastic angina (43). Moreover, it has been recently reported that hydroxyfasudil may be effective for the treatment of pulmonary hypertension (44). Indeed, Rho-kinase inhibitors may be useful for the treatment of a wide range of cardiovascular diseases (10). The present study suggests that Rho-kinase inhibitors may also be useful for the treatment of coronary I/R injury in humans.

Acknowledgment

We thank Y. Matsuo for excellent technical assistance in this study.

Reprint requests and correspondence: Dr. Toyotaka Yada, Kawasaki Medical School, 577 Matsushima, Kurashiki, Okayama, 701-0192, Japan. E-mail: yada@me.kawasaki-m.ac.jp.

REFERENCES

1. Vanbenthuysen PJ, McMurtry IF, Horwitz LD, et al. Reperfusion after acute coronary occlusion in dogs impairs endothelium-dependent relaxation to acetylcholine and augments contractile reactivity in vitro. J Clin Invest 1987;79:265–74.
2. Pearson PJ, Schaff HV, Vanhoutte PM, et al. Acute impairment of endothelium-dependent relaxations to aggregating platelets following reperfusion injury in canine coronary arteries. Circ Res 1990; 67:385–93.
3. Mehta JL, Nichols WW, Donnelly WH, et al. Impaired canine coronary vasodilator response to acetylcholine and bradykinin after occlusion-reperfusion. Circ Res 1989;64:43–54.

4. Defily DV, Chilian WM. Preconditioning protects coronary arteriolar endothelium from ischemia-reperfusion injury. Am J Physiol 1993; 265:H700–6.
5. Vanhoutte PM, Shimokawa H. Endothelium-derived relaxing factor and coronary spasm. Circulation 1989;80:1–9.
6. Korthuis RJ, Granger DN, Townsley MI, et al. The role of oxygen-derived free radicals in ischemia-induced increases in canine skeletal muscle vascular permeability. Circ Res 1985;57:599–609.
7. Olafsson B, Forman MB, Puett DW, et al. Reduction of reperfusion injury in the canine preparation by intracoronary adenosine: importance of the endothelium and the no-reflow phenomenon. Circulation 1987;76:1135–45.
8. Lamping KG, Marcus ML, Dole WP. Removal of endothelium potentiates canine large coronary artery constrictor response to 5-hydroxytryptamine in vivo. Circ Res 1985;57:46–54.
9. Cohen RA, Shepherd JT, Vanhoutte PM. 5-hydroxytryptamine can mediate endothelium-dependent relaxation of coronary arteries. Am J Physiol 1983;245:H1077–80.
10. Shimokawa H. Rho-kinase as a novel therapeutic target in treatment of cardiovascular diseases. J Cardiovasc Pharmacol 2002;39:319–27.
11. Shimokawa H, Seto M, Katsumata N, et al. Rho-kinase-mediated pathway induces enhanced myosin light chain phosphorylations in a swine model of coronary artery spasm. Cardiovasc Res 1999;43: 1029–39.
12. Kandabashi T, Shimokawa H, Miyata K, et al. Inhibition of myosin phosphatase by upregulated Rho-kinase plays a key role for coronary artery spasm in a porcine model with interleukin-1β. Circulation 2000;101:1319–23.
13. Takemoto M, Sun J, Hiroki J, et al. Rho-kinase mediates hypoxia-induced downregulation of endothelial nitric oxide synthase. Circulation 2002;106:57–62.
14. Satoh S, Utsunomiya T, Tsurui K, et al. Pharmacological profile of hydroxy fasudil as a selective Rho-kinase inhibitor on ischemic brain damage. Life Sci 2001;69:1441–53.
15. Yada T, Hiramatsu O, Kimura A, et al. In vivo observation of subendocardial microvessels of the beating porcine heart using a needle-probe videomicroscope with a CCD camera. Circ Res 1993; 72:939–46.
16. Mori HS, Haruyama Y, Shinozaki H, et al. New nonradioactive microspheres and more sensitive X-ray fluorescence to measure regional blood flow. Am J Physiol 1992;263:H1946–57.
17. Laufs U, Fata VL, Liao JK. Inhibition of 3-hydroxy-3-methylglutaryl (HMG)-CoA reductase blocks hypoxia-mediated down-regulation of endothelial nitric oxide synthase. J Biol Chem 1997;272:31725–9.
18. Katsura M, Mohri Y, Shuto K, et al. Up-regulation of L-type voltage-dependent calcium channels after long term exposure to nicotine in cerebral cortical neurons. J Biol Chem 2002;277:7979–88.
19. Ogita H, Node K, Asanuma H, et al. Amelioration of ischemia- and reperfusion-induced myocardial injury by the selective estrogen receptor modulator, raloxifene, in the canine heart. J Am Coll Cardiol 2002;40:998–1005.
20. Yada T, Shimokawa H, Hiramatsu O, et al. Hydrogen peroxide, an endogenous EDHF, plays an important role in coronary autoregulation in vivo. Circulation 2003;107:1040–5.
21. Ehring T, Krajcar M, Baumgart D, et al. Cholinergic and α-adrenergic coronary constriction with increasing ischemia-reperfusion injury. Am J Physiol 1995;268:H886–94.
22. Lamping KG. Enhanced contractile mechanisms in vasospasm: is endothelial dysfunction the whole story? Circulation 2002;105: 1520–2.
23. Golino P, Ashton JH, Buja LM, et al. Local platelet activation causes vasoconstriction of large epicardial canine arteries in vivo: thromboxane A2 and serotonin are possible mediators. Circulation 1989;79: 154–66.
24. Chitaley K, Webb RC. Nitric oxide induces dilation of rat aorta via inhibition of Rho-kinase signaling. Hypertension 2002;39:438–42.
25. Sauzeau V, Le Jeune H, Cario-Toumaniantz C. Cyclic GMP-dependent protein kinase signaling pathway inhibits RhoA-induced Ca^{++} sensitization of contraction in vascular smooth muscle. Biol Chem 2000;275:21722–9.
26. Sawada N, Itoh H, Yamashita J, et al. Cyclic GMP-dependent protein kinase phosphorylates and inactivates RhoA. Biochem Biophys Res Commun 2001;280:798–805.
27. Ikeda Y, Lindon HY, Lefer AM. Rosuvastatin, a new HMG-CoA reductase inhibitor, protects ischemic reperfused myocardium in normocholesterolemic rats. J Cardiovasc Pharmacol 2003;41:649–56.
28. Amin-Hanjani S, Stagliano NE, Yamada M, et al. Mevastatin, an HMG-CoA reductase inhibitor, reduces stroke damage and upregulates endothelial nitric oxide synthase in mice. Stroke 2001;32:980–6.
29. Arai M, Sasaki Y, Nozawa R. Inhibition by the protein kinase inhibitor HA1077 of the activation of NADPH oxidase in human neutrophils. Biochem Pharmacol 1993;46:1487–90.
30. Yada T, Hiramatsu O, Kimura A, et al. Direct in vivo observation of subendocardial arteriolar responses during reactive hyperemia. Circ Res 1995;77:622–31.
31. Murry CE, Jennings RB, Reimer KA. Preconditioning with ischemia: a delay of lethal cell injury in ischemic myocardium. Circulation 1986;74:1124–36.
32. Cohen MV, Liu GS, Downey JM. Preconditioning causes improved wall motion as well as smaller infarcts after transient coronary occlusion in rabbits. Circulation 1991;84:341–9.
33. Post H, Schulz R, Behrends M, et al. No involvement of endogenous nitric oxide in classical ischemic preconditioning in swine. J Mol Cell Cardiol 2000;32:725–33.
34. Nakano A, Liu GS, Heusch G. Exogenous nitric oxide can trigger a preconditioning state through a free radical mechanism, but endogenous nitric oxide is not a trigger of classical ischemic preconditioning. J Mol Cell Cardiol 2000;32:1159–67.
35. Kida M, Fujiwara H, Ishida M, et al. Ischemic preconditioning preserves creatine phosphate and intracellular pH. Circulation 1991; 84:2495–503.
36. Mohri M, Shimokawa H, Hirakawa Y, et al. Rho-kinase inhibition with intracoronary fasudil prevents myocardial ischemia in patients with coronary microvascular spasm. J Am Coll Cardiol 2003;41:15–9.
37. Wolfrum S, Dendorfer A, Rikitake Y, et al. Inhibition of rho-kinase leads to rapid activation of phosphatidylinositol 3-kinase/protein kinase akt and cardiovascular protection. Arterioscler Thromb Vasc Biol 2004;24:1–6.
38. Williams MW, Taft CS, Ramnauth S, et al. Endogenous nitric oxide (NO) protects against ischaemia-reperfusion injury in the rabbit. Cardiovasc Res 1995;30:79–86.
39. Hoshida S, Yamashita N, Igarashi J, et al. Nitric oxide synthase protects the heart against ischemia-reperfusion injury in rabbits. J Pharmacol Exp Ther 1995;274:413–8.
40. Jones SP, Girod WG, Palazzo AJ, et al. Myocardial ischemia-reperfusion injury is exacerbated in absence of endothelial cell nitric oxide synthase. Am J Physiol 1999;276:H1567–73.
41. Utsunomiya T, Satoh S, Ikegaki I, et al. Antianginal effects of hydroxyfasudil, a Rho-kinase inhibitor, in a canine model of effort angina. Br J Pharmacol 2001;134:1724–30.
42. Shimokawa H, Hiramori K, Iinuma H, et al. Anti-anginal effect of fasudil, a Rho-kinase inhibitor, in patients with stable effort angina: a multicenter study. J Cardiovasc Pharmacol 2002;40:751–61.
43. Masumoto A, Mohri M, Shimokawa H, et al. Suppression of coronary artery spasm by the Rho-kinase inhibitor fasudil in patients with vasospastic angina. Circulation 2002;105:1545–7.
44. Abe K, Shimokawa H, Morikawa K, et al. Long-term treatment with a Rho-kinase inhibitor improves monocrotaline-induced fatal pulmonary hypertension in rats. Circ Res 2004;94:385–93.

Am J Physiol Heart Circ Physiol 288: H1444–H1450, 2005.
First published November 11, 2004; doi:10.1152/ajpheart.00266.2004.

Adrenomedullin enhances therapeutic potency of bone marrow transplantation for myocardial infarction in rats

Takafumi Fujii,[1] Noritoshi Nagaya,[2,3] Takashi Iwase,[2] Shinsuke Murakami,[2] Yoshinori Miyahara,[1] Kazuhiro Nishigami,[3] Hatsue Ishibashi-Ueda,[5] Mikiyasu Shirai,[1] Takefumi Itoh,[2] Kozo Ishino,[6] Shunji Sano,[6] Kenji Kangawa,[4] and Hidezo Mori[1]

Departments of [1]Cardiac Physiology, [2]Regenerative Medicine and Tissue Engineering, [3]Internal Medicine, [4]Biochemistry, and [5]Pathology, National Cardiovascular Center, Osaka; and [6]Department of Cardiovascular Surgery, Okayama University Medical School, Okayama, Japan

Submitted 18 March 2004; accepted in final form 19 October 2004

Fujii, Takafumi, Noritoshi Nagaya, Takashi Iwase, Shinsuke Murakami, Yoshinori Miyahara, Kazuhiro Nishigami, Hatsue Ishibashi-Ueda, Mikiyasu Shirai, Takefumi Itoh, Kozo Ishino, Shunji Sano, Kenji Kangawa, and Hidezo Mori. Adrenomedullin enhances therapeutic potency of bone marrow transplantation for myocardial infarction in rats. *Am J Physiol Heart Circ Physiol* 288: H1444–H1450, 2005. First published November 11, 2004; doi: 10.1152/ajpheart.00266.2004.—Adrenomedullin (AM), a potent vasodilator, induces angiogenesis and inhibits cell apoptosis through the phosphatidylinositol 3-kinase/Akt pathway. Transplantation of bone marrow-derived mononuclear cells (MNC) induces angiogenesis. We investigated whether infusion of AM enhances the therapeutic potency of MNC transplantation in a rat model of myocardial infarction. Immediately after coronary ligation, bone marrow-derived MNC (5×10^6 cells) were injected into the ischemic myocardium, followed by subcutaneous administration of 0.05 $\mu g \cdot kg^{-1} \cdot min^{-1}$ AM (AM-MNC group) or saline (MNC group) for 3 days. Another two groups of rats received subcutaneous administration of AM alone (AM group) or saline (control group). Hemodynamic and histological analyses were performed 4 wk after treatment. Cardiac infarct size was significantly smaller in the MNC and AM groups than in the control group. A combination of AM infusion and MNC transplantation demonstrated a further decrease in infarct size. Left ventricular (LV) maximum change in pressure over time and LV fractional shortening were significantly improved only in the AM-MNC group. AM significantly increased capillary density in ischemic myocardium, suggesting the angiogenic potency of AM. AM infusion plus MNC transplantation demonstrated a further increase in capillary density compared with AM or MNC alone. Although MNC apoptosis was frequently observed 72 h after transplantation, AM markedly decreased the number of terminal deoxynucleotidyl transferase-mediated dUTP nick-end labeling-positive cells among the transplanted MNC. In conclusion, AM enhanced the angiogenic potency of MNC transplantation and improved cardiac function in rats with myocardial infarction. This beneficial effect may be mediated partly by the angiogenic property of AM itself and by its antiapoptotic effect on MNC.

angiogenesis; apoptosis; mononuclear cell

DESPITE THE RECENT REMARKABLE progress in medical and surgical treatment for ischemic heart disease, this disease remains a major cause of death worldwide (5). Bone marrow-derived mononuclear cells (MNC) contain various kinds of cell lineages and numerous cytokines that contribute to neovascularization (1, 15). In fact, autologous transplantation of bone marrow cells has been shown to enhance angiogenesis and improve cardiac function in an animal model of cardiac ischemia (6, 9, 10). Recent human studies have demonstrated beneficial effects of transplanted MNC in patients with ischemic heart disease (23, 25). However, some patients fail to respond to this cell therapy. Thus a novel therapeutic strategy to enhance the angiogenic property of MNC is desirable.

Adrenomedullin (AM) is a potent vasodilator peptide that was originally isolated from human pheochromocytoma (8). We have shown that infusion of AM has beneficial hemodynamic and renal effects in patients with heart failure (17). On the other hand, AM has been shown to activate the phosphatidylinositol 3-kinase (PI3-kinase)/Akt-dependent pathway in vascular endothelial cells, which is considered to regulate multiple critical steps in angiogenesis including endothelial cell proliferation, migration, and capillary-like formation (14, 22). In fact, we have shown that AM gene transfer induces therapeutic angiogenesis in a rabbit model of hindlimb ischemia via activation of Akt (24). These findings suggest that AM may play an important role in the regulation of vascular regeneration. In addition, AM has been shown to exert an antiapoptotic effect on a variety of cells including vascular endothelial cells (7, 20). Taking these findings together, combination therapy with MNC transplantation and AM infusion may have additional or synergetic effects on therapeutic angiogenesis for the treatment of ischemic heart disease.

Thus the purposes of this study were *1*) to investigate whether infusion of AM enhances the angiogenic potency of MNC transplantation in a rat model of myocardial infarction, and *2*) to investigate the effects of AM on survival and differentiation of the transplanted MNC to examine the underlying mechanisms of the effects induced by AM.

MATERIALS AND METHODS

Animal model. Myocardial infarction was produced in male Lewis rats weighing 200–220 g by left coronary ligation. In brief, after rats were anesthetized by intraperitoneal injection of pentobarbital sodium (30 mg/kg body wt), they were ventilated artificially. The heart was exposed via left thoracotomy, and the left coronary artery was ligated 2–3 mm from its origin between the pulmonary artery conus and the left atrium using a 6-0 proline suture. Finally, the heart was restored to its normal position, and the chest was closed. The Animal Care Committee of the National Cardiovascular Center approved this experimental protocol.

Address for reprint requests and other correspondence: N. Nagaya, Dept. of Regenerative Medicine and Tissue Engineering, National Cardiovascular Center Research Institute, 5-7-1 Fujishirodai, Suita, Osaka 565-8565, Japan (E-mail: nnagaya@ri.ncvc.go.jp).

The costs of publication of this article were defrayed in part by the payment of page charges. The article must therefore be hereby marked "*advertisement*" in accordance with 18 U.S.C. Section 1734 solely to indicate this fact.

Preparation of MNC. After Lewis rats were killed, bone marrow from the femur and tibia was collected and put in PBS. Marrow cells were loaded on a 1.077 gradient of Ficoll (Lymphoprep; Nycomed Pharma, Oslo, Norway) and centrifuged at 1,500 rpm for 20 min. The cells were then washed with 10 ml PBS to remove the Ficoll and centrifuged at 2,000 rpm for 10 min. The cells were finally suspended in PBS at a concentration of 5×10^6 cells in 50 μl PBS for transplantation. Fluorescence-activated cell sorting analysis demonstrated that 22 ± 1% of MNC were positive for lectin from ulex europaeus (UEA)-1 lectin (Sigma, St. Louis, MO).

MNC transplantation and AM infusion. Transplantation of bone marrow-derived MNC and/or 3-day infusion of AM was performed immediately after coronary ligation. MNC (5×10^6 cells in 50 μl PBS) were injected into the myocardium at five points in the border zone surrounding the infarct by using a 27-gauge needle. Recombinant human AM (0.05 $\mu g \cdot kg^{-1} \cdot min^{-1}$) was subcutaneously administered by using an osmotic minipump (model 2004; Alza, Palo Alto, CA) for 3 days. The pump was positioned in a pocket constructed in the subcutaneous tissue just below the subscapular region. For control, 5% glucose was infused in a similar manner in the rats receiving coronary ligation. This protocol resulted in the creation of four groups: *1*) AM infusion plus MNC transplantation (AM-MNC group, $n = 15$), *2*) vehicle infusion plus MNC transplantation (MNC group, $n = 14$), *3*) AM infusion plus PBS injection (AM group, $n = 14$), and *4*) vehicle infusion plus PBS injection (control group, $n = 13$).

Echocardiographic studies. Echocardiographic studies were performed 4 wk after surgery using a 7.5-MHz phased-array transducer (model HP SONOS 5500; Hewlett-Packard, Andover, MA). Rats were anesthetized by intraperitoneal injection of pentobarbital sodium (30 mg/kg body wt) as a supplement to maintain mild anesthesia. M-mode tracings were obtained at the level of the papillary muscles. Anterior and posterior end-diastolic wall thickness, left ventricular (LV) end-diastolic and end-systolic dimension, and LV fractional shortening were measured from three consecutive cardiac cycles by the American Society for Echocardiology leading-edge method (21).

Cardiac catheterization. Cardiac catheterization was performed 4 wk after surgery. Rats were anesthetized with intraperitoneal pentobarbital and placed on a heating pad to maintain body temperature at 37–38°C throughout the study. A 1.5 Fr micronanometer-tipped catheter was inserted in the right carotid artery for measurement of heart rate and mean arterial pressure. The catheter was then advanced into the LV for measurement of LV end-diastolic pressure and then replaced with a thermomicroprobe for measurements of cardiac output. These hemodynamic variables were measured with a pressure transducer (UFI, Morro Bay, CA) connected to a polygraph and recorded with a thermal recorder (model 7758 B system; Hewlett-Packard).

Infarct size measurement. After completion of hemodynamic measurements, the heart was arrested by an injection of 2 mmol KCl through the carotid artery, and the cardiac ventricles were excised. The size of myocardial infarction was determined by a previously described method (2). In brief, incisions were made in the LV so that the tissue could be pressed flat. The circumference of the entire flat LV and the visualized infarcted area, as judged from both the epicardial and endocardial sides, was outlined on a clear plastic sheet. The difference in weight between the two marked areas on the sheet was used to determine infarction size and was expressed as a percentage of LV surface area.

Histological analysis of microvessel density. LV myocardium was fixed in 10% formalin. Three cross sections of the LV, cut from apex to base, were obtained from individual rats for comparison among four groups ($n = 5$ each). They were embedded in paraffin and stained with Masson's trichrome for measurement of interstitial fibrosis. In other rats ($n = 5$ each), LV myocardium was embedded in optimum cutting temperature (OCT) compound (Sakura Finetechnical, Tokyo, Japan), snap frozen in liquid nitrogen, and cut into 5-μm-thick sections. Tissue sections were stained for alkaline phosphatase with an indoxyltetrazolium method to detect capillary endothelial cells ($n = 5$ in each group). The number of capillary vessels was counted in the peri-infarct area (a 1.0-mm band next to the scar) excluding scar region using a light microscope at a magnification of ×200. The numbers in five high-power fields in each rat were averaged and expressed as the number of capillary vessels. These morphometric studies were performed by two examiners who were blinded to treatment.

Detection of MNC apoptosis. To examine the antiapoptotic effect of AM on transplanted MNC, red fluorescence-labeled MNC were transplanted into ischemic myocardium in rats with ($n = 5$) and without ($n = 5$) AM infusion. Before implantation into the ischemic heart, suspended MNC were labeled with fluorescent dyes with a PKH26 (Red Fluorescent Cell Linker Kit; Sigma), as reported previously (13). AM was subcutaneously administered by using a minipump for 3 days. Rats were killed 72 h after MNC transplantation. The LV was enucleated, and muscle samples were embedded in OCT compound and snap frozen in liquid nitrogen for the detection of apoptosis. Serial sections of the heart were stained by terminal deoxynucleotidyl transferase-mediated dUTP nick-end labeling (TUNEL) for apoptosis using an in situ apoptosis detection kit (model S7111 Apoptag Fluorescein Kit; Intergen). Apoptosis of transplanted MNC was also evaluated by the detection of cleaved caspase-3-positive cells. In brief, the frozen tissue sections were incubated with anticleaved caspase-3 antibody (Cell Signaling), followed by incubation with FITC-conjugated IgG antibody (BD Pharmingen, San Diego, CA). The number of TUNEL/PKH26 double-positive cells and caspase-3/PKH26 double-positive cells was counted in 10 fields of each rat using a confocal microscopy (Fluoview model 500; Olympus, Tokyo, Japan).

The antiapoptotic effect of AM on MNC was also evaluated by in vitro TUNEL assay. MNC were plated on 12-well plates (1×10^6 cells per well) and cultured in serum-free medium for 24 h with control buffer, AM (1×10^{-7} M), or AM plus wortmannin, a PI3-kinase inhibitor (50 nM). Randomly selected microscopic fields ($n = 10$) were evaluated for calculating the ratio of TUNEL-positive cells to total cells.

Monitoring of implanted MNC in ischemic heart. Additional rats were used to examine whether transplanted MNC differentiate into endothelial cells, cardiomyocytes, vascular smooth muscle cells, or macrophages in the ischemic heart. PKH26 (red fluorescence)-labeled MNC were injected into the ischemic heart in rats with ($n = 8$) and without ($n = 8$) AM infusion. These subgroups of rats were killed 4 wk after coronary ligation. To identify vascular endothelial cells in vivo, FITC-labeled UEA-1 lectin was intravenously administered 30 min before the rats were killed ($n = 5$ in each group). The LV was enucleated, and muscle samples were then embedded in OCT compound, snap frozen in liquid nitrogen, and cut into sections. Sections were counterstained with 4′,6′-diamidino-2-phenylindole (DAPI) to detect nuclei. The number of DAPI/PKH26 double-positive cells and lectin-positive cells in the peri-infarct area was counted in 10 fields of each rat using a confocal microscopy. Frozen sections from other rats ($n = 3$ in each group) were incubated with mouse anticardiac troponin T (Novocastra, Newcastle, UK), anti-α-smooth muscle actin antibody (Dako, Copenhagen, Denmark), and anti-ED1 antibody (Serotec, Oxford, UK), followed by incubation with FITC-conjugated IgG antibody. In other rats (MNC group, $n = 5$; AM-MNC group, $n = 5$), the cardiac muscle from base to apex was transversely cut into 6-μm slices to calculate the number of transplanted MNC present within the heart 4 wk after transplantation. These morphometric studies were performed by two examiners who were blinded to treatment.

Statistical analysis. Numerical values were expressed as means ± SE. Comparisons of parameters among the four groups were performed by one-way ANOVA, followed by Newman-Keuls test for unpaired data. Comparisons of parameters between two groups were made by unpaired Student's *t*-test. A value of $P < 0.05$ was considered significant.

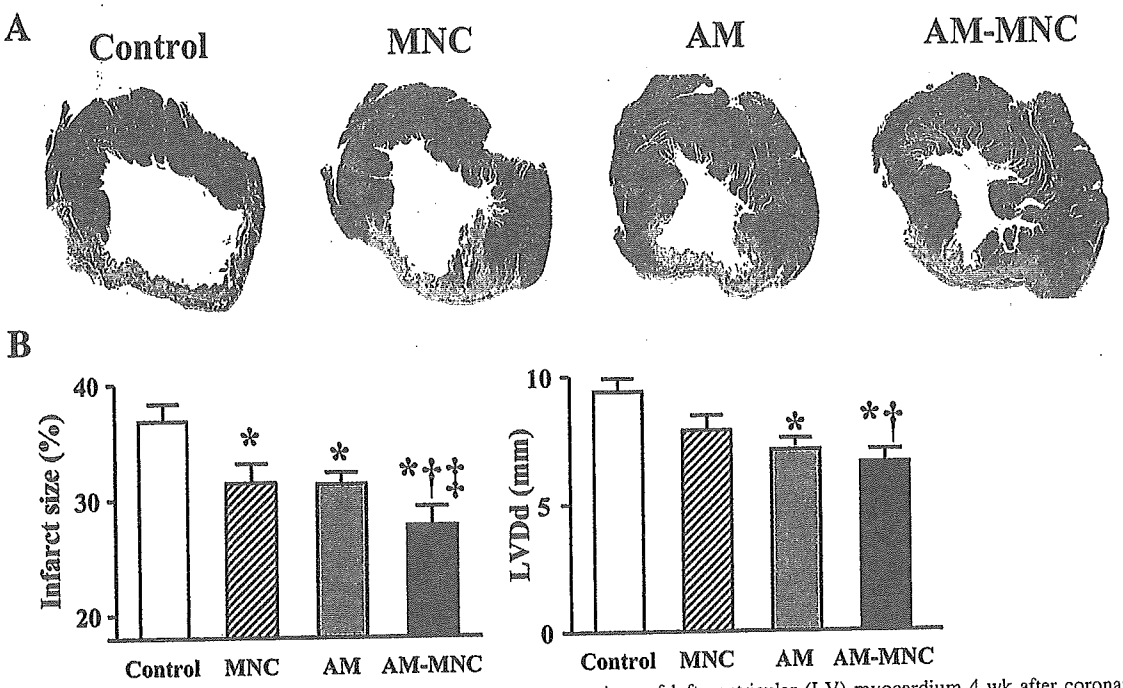

Fig. 1. *A*: representative examples of Masson trichrome-staining of transverse sections of left ventricular (LV) myocardium 4 wk after coronary ligation. *B*: quantitative analysis of infarct size and LV chamber size. Infarcted area and LV end-diastolic diameter (LVDd) of the adrenomedullin-mononuclear cell (AM-MNC) group were significantly smaller than those of the other groups. Values are means ± SE. *$P < 0.05$ vs. control; †$P < 0.05$ vs. MNC; ‡$P < 0.05$ vs. AM.

RESULTS

Infarct size and ventricular weight. Moderate-to-large infarcts were observed in the control group after coronary ligation (Fig. 1). However, infarct size was smaller in the MNC, AM, and AM-MNC groups than in the control group. In particular, it was very small in the AM-MNC group. Quantitative analysis also demonstrated that cardiac infarct size in the AM-MNC group was smallest among the four groups. Right ventricular weight was significantly lower in the AM and AM-MNC groups than that in the control group (Table 1). LV weight did not significantly differ among the four groups.

Echocardiographic findings. LV diastolic dimension was smallest in the AM-MNC group, followed by the AM, MNC, and control groups (Fig. 1). LV fractional shortening in the AM-MNC group was also higher than that in the control, MNC, and AM groups (Table 2). Diastolic thickness of the anterior wall was significantly attenuated in the MNC, AM, and AM-MNC groups compared with the control group.

Hemodynamics. Cardiac output in the AM-MNC group was significantly higher than that in the control, MNC, and AM groups (Fig. 2). LV end-diastolic pressure in the MNC, AM, and AM-MNC groups was significantly lower than that in the control group. LV maximum change in pressure over time (dP/d*t*) in the MNC and AM-MNC group were significantly higher than that in the control group. Similarly, LV minimum dP/d*t* was significantly decreased only in the AM-MNC group.

Capillary density. Alkaline phosphatase staining of ischemic myocardium showed marked augmentation of neovascularization in the MNC, AM, and AM-MNC groups compared with the control group (Fig. 3*A*). Quantitative analysis demonstrated that capillary density was significantly higher in the AM-MNC group than in the MNC and AM groups (Fig. 3*B*). Cartilage, bone, or fat was not observed in the transplanted area. No tumor-like cells were seen.

Antiapoptotic effect of AM on MNC. Red fluorescence-labeled MNC were detected in each recipient heart 72 h after transplantation (Fig. 4). TUNEL-positive cells were frequently observed in the MNC group. In contrast, these apoptotic cells

Table 1. *Physiological profiles of four experimental groups*

	Control	MNC	AM	AM-MNC
Number	13	14	14	15
Body weight, g	274±3	285±5	287±3	305±4*
Heart rate, bpm	410±24	404±30	398±33	387±36
MAP, mmHg	101±11	104±13	103±9	116±14*
LV wt/body wt, g/kg	2.4±0.2	2.5±0.2	2.6±0.1	2.5±0.2
RV wt/body wt, g/kg	1.1±0.1	0.9±0.1	0.8±0.1*	0.7±0.1*

Values are means ± SE; number is number of rats in each group. Control group, myocardial infarction rats given vehicle; MNC group, those given mononuclear cells; AM, those given adrenomedullin; AM-MNC, those given AM and MNC; MAP, mean arterial pressure; LV, left ventricle; RV, right ventricle. *$P < 0.05$ vs. control.

Table 2. *Echocardiographic findings*

	Control	MNC	AM	AM-MNC
LVDd, mm	9.9±0.2	8.3±0.3	7.3±0.2*	6.9±0.3*†
LVDs, mm	8.4±0.3	6.6±0.4	5.8±0.2*	5.1±0.2*
%FS, %	14±1	22±1*	21±1*	26±1*†‡
AWT diastole, mm	1.0±0.2	1.3±0.3*	1.3±0.3*	1.4±0.4*
PWT diastole, mm	1.5±0.5	2.2±0.4	2.1±0.4	2.2±0.4

Values are means ± SE. LVDd, LV diastolic dimension; LVDs, LV systolic dimension; %FS, LV fractional shortening; AWT, anterior wall thickness; PWT, posterior wall thickness. *$P < 0.05$ vs. control; †$P < 0.05$ vs. MNC; ‡$P < 0.05$ vs. AM.